(ATINER)

Athens Journal of Sciences

(ATINER)

# Volume 7, Issue 3, September 2020
# Articles

## Mission

ATINER is an Athens-based World Association of Academics and Researchers based in Athens. ATINER is an independent and non-profit **Association** with a **Mission** to become a forum where Academics and Researchers from all over the world can meet in Athens, exchange ideas on their research and discuss future developments in their disciplines, **as well as engage with professionals from other fields**. Athens was chosen because of its long history of academic gatherings, which go back thousands of years to *Plato's Academy* and *Aristotle's Lyceum.* Both these historic places are within walking distance from ATINER's downtown offices. Since antiquity, Athens was an open city. In the words of Pericles, **Athens*"...is open to the world, we never expel a foreigner from learning or seeing".*** **(**"Pericles' Funeral Oration", in Thucydides, *The History of the Peloponnesian War).* It is ATINER's **mission** to revive the glory of Ancient Athens by inviting the World Academic Community to the city, to learn from each other in an environment of freedom and respect for other people's opinions and beliefs. After all, the free expression of one's opinion formed the basis for the development of democracy, and Athens was its cradle. As it turned out, the Golden Age of Athens was in fact, the Golden Age of the Western Civilization. *Education* and *(Re)searching* for the 'truth' are the pillars of any free (democratic) society. This is the reason why *Education* and *Research* are the two core words in ATINER's name.

The Athens Journal of Sciences
ISSN NUMBER: 2241-8466- DOI: 10.30958/ajs
Volume 7, Issue 3, September 2020
Download the entire issue (PDF)

# Athens Journal of Sciences
# Editorial and Reviewers' Board

# President's Message

All ATINER's publications including its e-journals are open access without any costs (submission, processing, publishing, open access paid by authors, open access paid by readers etc.) and is independent of presentations at any of the many small events (conferences, symposiums, forums, colloquiums, courses, roundtable discussions) organized by ATINER throughout the year and entail significant costs of participating. The intellectual property rights of the submitting papers remain with the author. Before you submit, please make sure your paper meets the basic academic standards, which includes proper English. Some articles will be selected from the numerous papers that have been presented at the various annual international academic conferences organized by the different divisions and units of the Athens Institute for Education and Research. The plethora of papers presented every year will enable the editorial board of each journal to select the best, and in so doing produce a top-quality academic journal. In addition to papers presented, ATINER will encourage the independent submission of papers to be evaluated for publication.

The current issue is the third of the seventh volume of the *Athens Journal of Sciences (AJS)*, published by Natural & Formal Sciences Division of ATINER.

Gregory T. Papanikos, President, ATINER.

# Athens Institute for Education and Research

*A World Association of Academics and Researchers*

**9th Annual International Conference on Chemistry**
**19-22 July 2021, Athens, Greece**

The Chemistry Unit of ATINER, will hold its **9th Annual International Conference on Chemistry, 19-22 July 2021, Athens, Greece** sponsored by the Athens Journal of Sciences. The aim of the conference is to bring together academics and researchers of all areas of chemistry and other related disciplines. You may participate as stream organizer, presenter of one paper, chair a session or observer. Please submit a proposal using the form available (https://www.atiner.gr/2021/FORM-CHE.doc).

**Academic Members Responsible for the Conference**

- **Dr. Ellene Tratras Contis**, Head, Chemistry Unit, ATINER & Professor of Chemistry, Eastern Michigan University, USA.
- **Dr. Nicolas Abatzoglou**, Head, Environment Unit, ATINER & Professor, Department of Chemical & Biotechnological Engineering, University of Sherbrook, Canada, Chair Pfizer, PAT in Pharmaceutical Engineering, Director GREEN-TPV and GRTP-C & Pwelcomes.

**Important Dates**

- Abstract Submission: **21 December 2020**
- Acceptance of Abstract: 4 Weeks after Submission
- Submission of Paper: **21 June 2021**

**Social and Educational Program**

The Social Program Emphasizes the Educational Aspect of the Academic Meetings of Atiner.

- Greek Night Entertainment (This is the official dinner of the conference)
- Athens Sightseeing: Old and New-An Educational Urban Walk
- Social Dinner
- Mycenae Visit
- Exploration of the Aegean Islands
- Delphi Visit
- Ancient Corinth and Cape Sounion

**Conference Fees**

Conference fees vary from 400€ to 2000€
Details can be found at: https://www.atiner.gr/2019fees

**9th Annual International Conference on Physics**
**19-22 July 2021, Athens, Greece**

The Physics Unit of ATINER, will hold its **9th Annual International Conference on Physics, 19-22 July 2021, Athens, Greece** sponsored by the Athens Journal of Sciences. The aim of the conference is to bring together academics and researchers of all areas of physics and other related disciplines. Please submit a proposal using the form available (https://www.atiner.gr/2021/FORM-PHY.doc).

**Important Dates**

- Abstract Submission: **21 December 2020**
- Acceptance of Abstract: 4 Weeks after Submission
- Submission of Paper: **21 June 2021**

**Academic Member Responsible for the Conference**

- **Dr. Ethel Petrou**, Academic Member, ATINER & Professor and Chair, Department of Physics, Erie Community College-South, State University of New York, USA.
- **Dr. Bala Maheswaran**, Head, Electrical Engineering Unit, ATINER & Professor, Northeastern University, USA.

**Social and Educational Program**

The Social Program Emphasizes the Educational Aspect of the Academic Meetings of Atiner.

- Greek Night Entertainment (This is the official dinner of the conference)
- Athens Sightseeing: Old and New-An Educational Urban Walk
- Social Dinner
- Mycenae Visit
- Exploration of the Aegean Islands
- Delphi Visit
- Ancient Corinth and Cape Sounion

More information can be found here: https://www.atiner.gr/social-program

**Conference Fees**

Conference fees vary from 400€ to 2000€
Details can be found at: https://www.atiner.gr/2019fees

*Athens Journal of Sciences- Volume 7, Issue 3, September 2020 – Pages 127-142*

# Could Striate Cortex Microcolumns Serve as the Neural Correlates of Visual Consciousness?

*By Walter Alexander Escobar[*] & Megan Slemons[•]*

*Neural circuit structure studies commonly focus on cell connectivity within circuits and not on the 3-D structure of the circuit itself. In part, this is due to the difficulty of identifying the three-dimensional structure of circuits containing hundreds to thousands of cells. However, given the importance of structure-function relationships in biology, this approach may be missing valuable information related to the properties and activities of these circuits. A case in point being the well-known and studied striate cortex microcolumns found in several mammals. Within the Quantized Visual Awareness (QVA) hypothesis, the specific topology of these microcolumns is thought to be a key factor in determining the type of qualia produced by these neural circuits of the visual cortex. This communication serves as a gentle reminder that we may be overlooking important features of the circuits we study in our rush to understand circuit activity and physiology, especially as it relates to the neural correlates of visual consciousness.*

**Keywords:** *Neural circuits, striate cortex microcolumns, visual awareness, visual consciousness*

## Introduction

Researchers have studied neural circuits across many species for decades. The models based on this research take into consideration the various currents ($K^+$, $Na^+$, $Ca^{++}$, etc.) that cross the membranes of neurons and the connectivity of these cells within their respective circuits. In these models, the physical shape of the neural circuit is not considered in the function of the circuit except in rudimentary ways.

As a result, we tend to think of specific circuit topology as noise or irrelevant variations that are not important in terms of the underlying biology. It may be the case that this is indeed true for many neural circuits but we should remain open to the idea that this may not always be true. One of the basic tenets of biology is that structure defines function and it is possible that in certain cases the specific 3-D topology of a circuit is functionally important.

A case in point is the microcolumn circuits we find in the striate cortex (V1) of certain mammals. The cells in this part of the cortex are known to process basic bits of information used for the production of visual experiences. However, the role of V1 in the production of the visual experience itself has remained controversial. Leopold and Logothetis observed that fewer cells in V1 seem to

[*]Senior Lecturer, Department of Biology, Emory University, USA.
[•]Library and IT Services, Center for Digital Scholarship, Woodruff Library, Emory University, USA.

respond to changes in perception when compared to V4, V5 or the inferior temporal cortex (Leopold and Logothetis 1996, Keliris et al. 2010). The authors interpreted this to indicate a lesser role for V1 in the production of conscious experiences. In other studies, patients with blindsight and a damaged V1 experienced phosphenes when transcranial magnetic stimulation (TMS) was applied to the parietal cortex (Mazzi et al. 2014), indicating that perhaps V1 is not necessary for visual experiences.

In contrast to these studies, the work of many researchers indicates that the recurrent activation of V1 from visual areas like V3, V4, and V5, correlates with the onset of phenomenal visual experiences (Boehler et al. 2008, Cowey and Walsh 2000, Kosslyn et al. 2001, Mehta et al. 2000, Overgaard et al. 2004, Pascual-Leone and Walsh 2001, Silvanto et al. 2005, Tong 2003). This work indicates that the recurrent activation of V1 by the higher centers (V3, V4, V5) is required for the production of visual experiences and when this recurrent activation is inhibited, there is a loss of conscious, visual content. On the whole, the evidence presented here supports the idea that V1 is required for the production of visual experiences.

The Quantized Visual Awareness model (QVA) proposes that V1 microcolumn circuits play a central role in the formation of subjective, visual experiences and it is their specific topology that leads to the production of small, discrete quanta of awareness (qualia) that are integrated into our visual field through temporal synchronization - a phenomenon correlated with conscious perception (Eckhorn et al. 1988, 1993, Eckhorn 1994, Fries et al. 1997, Kreiter and Singer 1996, Singer 1998). These quanta of awareness arise directly from the activation of microcolumns with the type of quale being determined by the specific topology of the microcolumn. Thus, the microcircuit topology is central to understanding what type of quale will be produced (Escobar 2013, 2016).

*Fine Structure of the Striate Cortex (V1)*

The striate cortex contains ocular dominance columns (ODCs) that correspond to specific points of the visual field (Hubel and Wiesel 1974, Hubel et al. 1978). All of the neural cells and circuits within a specific ODC are tuned to the same eccentricity and polar angle of the visual field and have the same ocular bias. We can think of each ODC as an organizing center used to process various attributes for a given point of the visual field. Within any given ODC there are 50-80 microcolumns (Mountcastle 2003, Peters and Sethares 1991) with diameters in the range of 30 micrometers (Figure 1). Each microcolumn is defined by the bundles of pyramidal cell apical dendrites placed through the center of each column (Peters and Walsh 1972). This anatomy suggests that these microcolumns may act as independent units and this is supported by the fact that there are inhibitory interneurons that line the edges of these columns and create what is known as an inhibitory fringe (Von Bonin and Mehler 1971). Thus, the activation of any given microcolumn inhibits nearby columns.

Early studies by Hubel and Wiesel seemed to indicate that microcolumns are tuned to different stimuli (Hubel and Wiesel 1974). Hubel and Wiesel saw

changes in tuning specificity in distances as small as 30 micrometers, possibly indicating that there was a change in tuning specificity as their electrode moved from one microcolumn to another. QVA predicts that microcolumns are tuned to various visual attributes like color and line orientation. Moreover, these microcolumns contain within their structure the information required to generate a bit of experience or a quale. This experience, by necessity, is very simple like sensing a bit of the color red at a certain point of your visual field. However, given that you have 50-80 microcolumns within each ODC, these simple qualia can be combined into more complex experiences by activating different sets of microcolumns within each ODC.

For the purpose of illustrating this concept, let us imagine that there are a few microcolumn topologies that correspond to color qualia. These might be red, blue, and green. These colored qualia can be combined in the classical sense to create new colors. For example, red and green can be combined to create the sensation of the color yellow in the same way that red and green lights combine additively to form the color yellow. To create the sensation of a vertical yellow line at a specific point in your visual field, you would activate microcolumns tuned to the vertical line orientation as well as red and green colors. In this fashion, it should be possible to generate the sensation of a large number of varied experiences by changing the combination and number of microcolumns contributing to the experience for each point of the visual field. One of the essential principles of QVA is that it allows for a tremendous amount of complexity to arise from the combination of otherwise simple subunits.

**Figure 1.** *A) Top of an Ocular Dominance Column (ODC). The Circles are the Tops of the Microcolumns contained within an ODC as shown in B). The Various Hues Correspond to Orientation Tuning Covering a Complete set of 180 Degrees. The Red, Blue and Green Microcolumns are used to Process Color. C) These Columns Pass through Blobs – Tissue that stains for Cytochrome Oxidase Activity and is tuned to Color Stimuli*

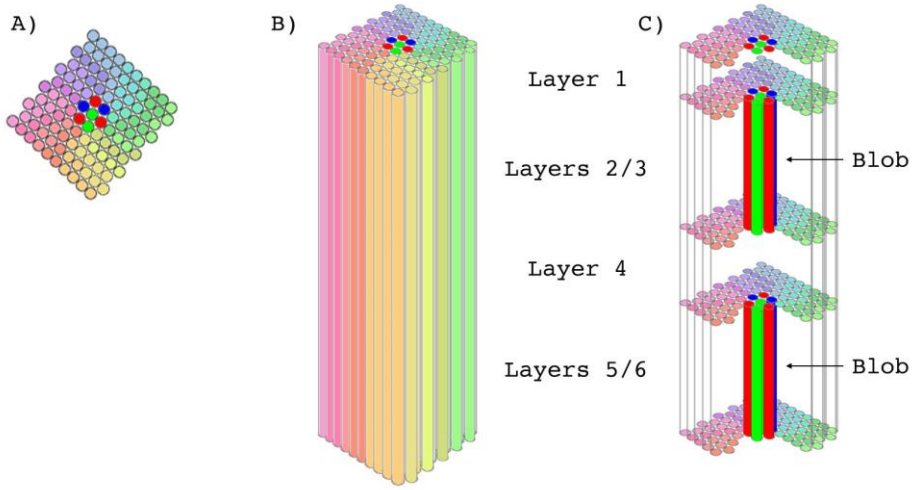


*Source:* Adapted from Escobar 2016.

Control over the activity of individual microcolumns is provided by the higher visual centers: V3, V4, and V5. Although there will be activity in V1 microcolumns produced by the incoming data from the eyes, this is not sufficient to induce a phenomenal experience. It is only by reaching gamma synchrony that these columns contribute to phenomenal consciousness (this is described in the Discussion section). Decisions made by V3, V4, and V5 will push the already active V1 microcolumns into gamma synchrony. Given that we are only shifting the activity of V1 microcolumns, these changes in activity may appear small when probed by electrophysiological techniques. Several studies looking at changes of neural activity as a function of changes in perception indicate that fluctuations in V1 activity are of a smaller scale than those seen for higher centers like V4 (Leopold and Logothetis 1996, Keliris et al. 2010).

Consider the phenomenon of color constancy. This occurs when parts of the visual scene are in shadow and the colors of objects within the shadow are made to appear lighter by our own visual system. This occurs so that we may see these objects as having the same color in diverse lighting conditions. Although the specific mechanism by which color constancy arises is not fully understood, this phenomenon must take place in V4 (Witzel and Gegenfurtner 2018). Information arriving at V1 from the eyes is retinotopic in nature (reflecting individual points of the visual field). It is impossible for the required comparisons in lighting to be made at this point in the feedforward sweep (forward movement of information through the visual system). It is only when this information arrives at V4 that distant points of the visual scene can be compared and illumination ratios determined for the scene.

Primed with this information, V4 determines which microcolumns of V1 should be pushed into gamma synchrony. Using the example of the yellow, vertical line above, V4 pushes microcolumns corresponding to red, green and vertical qualia into gamma synchrony while simultaneously activating triplets of red, blue and green qualia (equivalent to white) to lighten the color. Based on this example, we can see the higher visual centers (V3, V4, and V5) are playing a pivotal role in orchestrating the activity of V1 microcolumns and thereby determining which qualia are included in phenomenal consciousness. In most cases, however, these higher visual centers are not the physical location of the neural correlates of visual consciousness.

I have limited my discussion of qualia to just color and line orientation information, but for this hypothesis to be robust, there must be qualia that correspond to the sensations of depth, motion and other aspects of visual experience. QVA proposes that all of these visual properties are produced in the same fashion as that described above and therefore there must be unique microcircuit topologies that correspond to each of these properties.

Although there are millions of microcolumns in V1, QVA predicts there should be a limited set (50-100) of microcircuit topologies (with corresponding simple qualia), which can be combined into a large number of possible visual scenes. Thus, we would expect the same topologies to repeat throughout V1, with the same microcircuit topologies found in many ODCs. Also, these same microcolumn topologies would not be expected in other parts of the occipital

cortex (ex. V2, V3, V4, V5). Currently, there is no other model (cognitive or otherwise) that proposes there should be any repeating microcircuit topologies in the cortex. If this model holds true, it should be possible to look for these same circuit topologies in other animal models since it is likely some of the same microcircuit topologies are used throughout the animal kingdom. For the first time, we may be able to gain quantitative information about subjective experience in humans and animals.

QVA is rooted in the neuroanatomy of the striate cortex, relates well with studies investigating the onset of visual phenomenal experiences, and follows the fundamental principle of all biological systems – all complex biological systems are formed from the many subunits contributing to that system (a principle lacking from many current ideas about consciousness and subjective experience). In addition, this model provides bridging laws that explain how the activation of neural microcircuits is integrated and result in the production of our overall visual consciousness (Block 1996, Lamme 2003).

In an attempt to prime the search for circuits of V1 with repeating topologies we initiated a study of the structure of the striate cortex using images from the Human Brain Project (please see below for a description). These images provide an in-depth look at this tissue, though only in 2 dimensions. It is hoped that studies like these will inspire others to look at this same region with techniques that can probe the structure of these circuits in greater detail.

## Materials and Methods

We are using MINC files generated by the Human Brain Project (Amunts et al. 2013). These images can be accessed on the Human Brain Project website (https://www.humanbrainproject.eu/en/) - the resolution of the images is 20 microns per pixel. For this study, we received files of 10 micron resolution from Dr. Allan Evans and Claude Lepage in the Department of Neurology and Neurosurgery, Psychiatry and Biomedical Engineering, McGill University in Montreal, Canada.

### *Preparing the Original Files for Analysis*

The original brain scan images were stored as MINC (Medical Imaging NetCDF, file extension of .mnc) files - a medical image file format not readable by common image viewing and editing software such as Photoshop or Windows Photo Viewer. To convert these files into a usable format, we used two pieces of medical image software from the National Institutes of Health. We first used MIPAV (Medical Image Processing, Analysis, and Visualization) to convert the MINC files into TIFs, which were still unreadable in Photoshop due to an "unsupported bit depth". The files were then opened in ImageJ and saved as 16-bit TIFs, resulting in files that were readable in Photoshop. (Thank you to Michael Page for assistance with bit-depth troubleshooting.) The images were then cropped in Photoshop to the same extent showing just the relevant area of study on the

scans. Each image was marked with a common origin point from which to measure the distance of each observation. These images were annotated in Photoshop with each observation recorded as a single point with an ID number next to it. Further details on each observation were recorded in a separate spreadsheet.

## Results

In the cross sections shown of V1 and V2, it is apparent that there are large differences in the structure of local circuits within these regions (Figure 2). The cell clusters of V1 appear to be distinct and unique in their appearance while the corresponding cells of V2 are not and indeed look more like they are distributed in a random way. This is despite the fact that both V1 and V2 are known to contain complete retinotopic maps and cells of these centers only process local information for specific points of the visual field. Clearly the observed microcolumn structure of V1 is a distinguishing feature and must be important for the function of the striate cortex (V1).

**Figure 2.** *A) Human Left Hemisphere: Section 300 of The Big Brain Project (Amunts et al. 2013). Tissue was Nissl stained and then digitized (1.0-by-1.0 μm pixel size). This Slice through the Occipital Lobe Includes a Cross Section of V1 and V2. B) The Location of This Image is shown for Reference in A) and is found at the Bottom of the Calcarine Sulcus. Cortical Layer I is at the Top and Layer VI is at the Bottom of this Image. This Image is Representative of V1 Cell Distributions - Clusters of Cells (Especially in Layers V and VI) seem to Aggregate into Distinct Units. C) Please see A) for Location. This Image is Characteristic of Cell Distributions in V2. Notice the Lack of Cell Clusters and Lack of Cell Columns running from the Top (layer I) to Bottom (layer VI) as seen for V1. Brain Image Files were supplied by Alan Evans and Claude Lepage (McGill University) and the DSA MultiSlide Viewer used to Display These Images was developed by David Gutman (Emory University)*

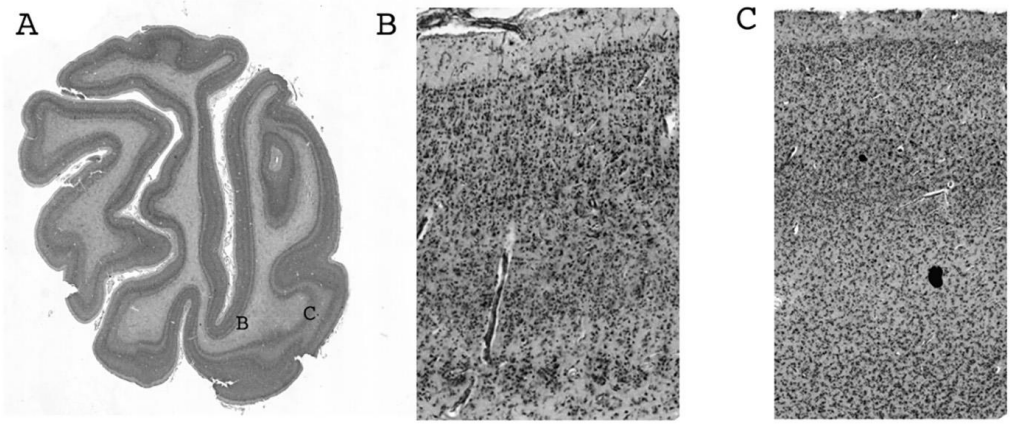


We were limited in our ability to see complete three-dimensional circuit structures since we were required to use two-dimensional (albeit detailed) images

of the brain. In addition, the Nissl stain only allows us to observe cell bodies in the images we use. Given these limitations, our first attempts to identify conserved or repeating circuit structures are confined to looking at cell clustering patterns in layers V and VI of the calcarine sulcus. It is hoped that the large amount of data will allow us to identify repeating cell clustering-patterns in this data and thus describe, in a cursory way, repeating circuit structures.

As observed in Figure 3, the cortical tissue lining the calcarine sulcus can be easily seen in these slices. By visually surveying cell clustering in layers V and VI we have found several cell-clustering patterns that do repeat in various slices (Figure 4). In identifying these patterns, we considered that they would not necessarily have the same orientation and could be rotated by as much as 180 degrees around their vertical or horizontal axis. Unfortunately, this variation in orientation increases the difficulty of identifying these patterns through pattern recognition software. Although we have just begun our studies, we have already identified several patterns as shown in Table 1 along with observed instances of these patterns in the slices available.

**Figure 3.** *A) Human Left Hemisphere: Section 301 of the Big Brain Project (Amunts et al. 2013). Tissue was Nissl stained and then digitized (10.0-by-10.0 μm Pixel Size). We Began our Survey of the Slices at the Arrow as indicated in the Image and scanned for Cell-Clustering Patterns*

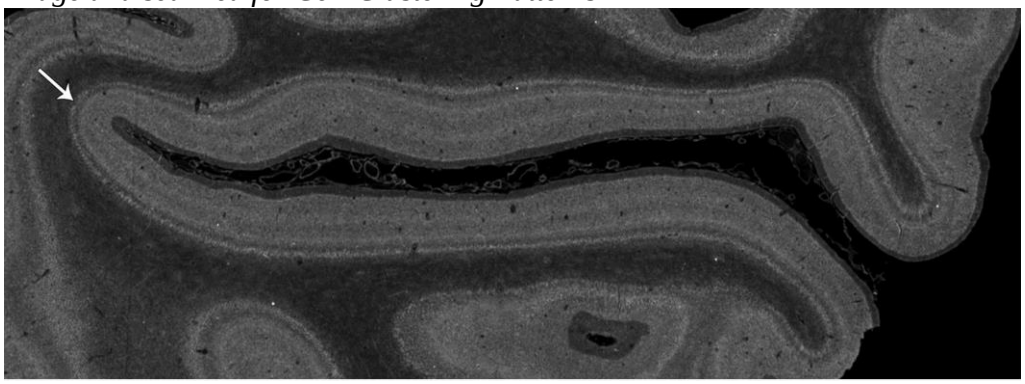

**Figure 4.** *A) Human Left Hemisphere: Section 301 of the Big Brain Project (Amunts et al. 2013). Tissue was Nissl stained and then digitized (10.0-by-10.0 μm Pixel Size). Clustering Patterns can be More Easily seen in this Magnified Image of Figure 3. Notice the Unique and Clearly Visible Cell Clustering Patterns found in Layers 5 and 6*

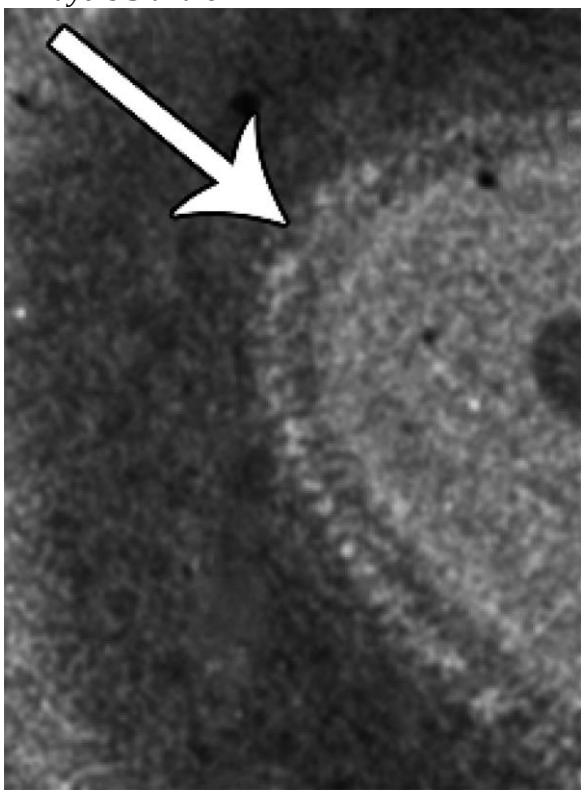

**Table 1.** *Microcircuit Cell-Clustering Patterns are labelled CP (Clustering Pattern) and numbered in the order that they were identified. Several Instances are shown for Each Type and the Slice of Origin is indicated over the Image of the Cell Clustering Pattern. Some of these Clustering Patterns Resemble Letter Shapes and we have given them Secondary Labels based on this Resemblance*

| Label -Primary - Secondary | CP1 "Lamedh" | CP2 "h" | CP3 "YY" | CP4 "ʒ" | CP5 "ω" | CP6 "κ" |
|---|---|---|---|---|---|---|
| Slice # | 298  | 300  | 298  | 300  | 298  | 298  |
| Slice # | 300  | 300  | 299  | 300  | 299  | 301  |
| Slice # | 300  | 300  | 300  | 300  | 300  | |
| Slice # | | 300  | 301  | | | |

It is understood that these clustering patterns could be parts of larger patterns that are yet to be discovered with a more robust analytical tool. Given that what we see are two-dimensional representations of three-dimensional patterns, it is also possible that some of the discrete patterns we observe could actually be part one larger circuit topology in three-dimensions. For the purposes of initiating this study, we are considering them as unique patterns for the time and until determined otherwise.

We plan to continue cataloging cell-clustering patterns that repeat and hope to have a more complete set in the near future. Our hope is to establish a set of cell clustering-patterns that could be used to train a pattern recognition system to identify them and look at larger swaths of V1.

## Discussion

A great degree of structure is easily observed when looking at microcolumns, specifically in layers V and VI of the striate cortex (Figure 4). Many have taken this structure to be of little importance since they believe the activity of these microcircuits only becomes significant at the level of larger populations of cells. Current attempts to understand the functional significance of the neural activity of the striate cortex use a statistical approach by populating large, in-silico circuits with specific cells types (amacrine, chandelier, etc.). The types and numbers of cells are based on known frequencies of these cells in the tissues of interest. Clearly, this approach completely disregards the true and natural structure of these circuits and treats this structure as immaterial (Muralidhar et al. 2014).

Giulio Tononi's Integrated Information Theory (IIT) gives no value to the structure of these cortical columns and completely bypasses the key biological principle that structure defines function. IIT frames information in a more abstract fashion that correlates with the information states of those parts of the brain contributing to consciousness and not with the specific structure of the brain or specific neural circuits of the brain (Tononi 2008, Tononi and Koch 2008). This theory is potent in that it leads to a belief that certain computer systems can be made aware based on their ability to process information dynamically through self-modulation. There is currently much momentum, funding and research based on these ideas. However, as a biologist, I believe this abstraction of the concept of information found in natural systems has completely left the realm of the true nature of the neural correlates of consciousness. It is true that biological systems do possess and store information, but without exception, in nature, this information takes the form of a definite biological structure or electrochemical gradients.

I have postulated the distinct microcolumn 3-D structures of V1 are significant for the production of individual quale and may be key to understanding how visual phenomenal experiences arise. The QVA hypothesis predicts that quanta of awareness (qualia) are incorporated into visual consciousness through the synchronous spiking of microcolumns. Thus, a microcolumn of a certain topology will reproducibly generate simple forms of awareness like the color red when it becomes active (Escobar 2013, 2016). By controlling which microcolumns

within an ocular dominance column become temporally synchronous, the higher centers (V3, V4, V5) can assign specific values for color, depth, orientation, and movement to individual points of the visual field.

The idea that the neural correlates of consciousness could be found in single columns of cells is not new. Francis Crick proposed that the smallest units of consciousness (a node) could be contained within a cortical column of cells (Crick and Koch 2003). In addition, Semir Zeki has suggested for years that there might be "microconsciousnesses" contained within neural networks of the visual cortex and that these "microconsciousnesses" are integrated to form our overall visual experience (Zeki and Bartels 1999, Yu and Zeki 2014, Zeki, 2015a, b).

*The Hard Problem*

Although we have focused solely on the structure of microcircuits, these microcircuits themselves are not the physical surrogate of qualia. QVA proposes the specifically shaped electromagnetic (EM) fields arising from active microcolumns are the physical aspect of qualia (Escobar 2013, 2016). This proposal is presented within the context of several others who have previously suggested EM fields serve as the surrogate of conscious experience (Pockett et al. 2009, John 2002, McFadden, 2002a, b, 2013). The topology of these small electromagnetic fields determines the unique type of quale that is produced. Moreover, given that these small fields arise in close proximity to each other, we can easily understand how these individual qualia integrate themselves into our larger visual experience. It is well known that nearby electric fields automatically integrate themselves into one larger field. Thus, individual qualia EM fields combine into one larger EM field that contains our visual subjective experience and more.

Electromagnetic fields are wave mechanical phenomena. Wave mechanical processes interfere with each other in what is known as constructive or destructive interference. This is illustrated when water wave troughs come together with wave crests and cancel each other out to create a relatively flat surface. This is an example of destructive interference. Two wave crests coming together to create an even larger crest is an example of constructive interference.

In most material objects, the electromagnetic fields of atoms and molecules interfere with each other in a random manner and this has the general effect of reducing the amplitude (destructive interference) of the integrated fields. This is why inanimate objects don't generally produce large electric or magnetic fields at the macroscopic level. In other words, you do not get a shock when you touch everyday objects or have iron containing materials tugged at by magnetic fields arising from the objects around you.

QVA postulates that the function of V1 microcolumns is to specifically shape EM fields through the constructive and destructive interference arising from various parts of the microcolumn. These specifically shaped microcolumn EM fields correspond to simple forms of awareness (like a point of the color red) that can serve as units for natural selection.

However, all of this does not answer the hard problem: Why are physical processes ever accompanied by experience (Chalmers 1995)? The answer to this comes from understanding that biological systems never create physical properties but use what is already present in nature to enhance reproductive success. For example, mammalian organisms did not invent diffusion but they use it to distribute molecular oxygen throughout their bodies. Organisms did not invent chemical reactions but they use them for their daily metabolism. Electromagnetism was part of nature long before biological systems came into existence and yet many organisms (ex. electric eels) have evolved to use electric or magnetic phenomena to enhance their survivability.

If it is the case that biological systems do not invent universal physical properties, we can reasonably ask, "could some fundamental form of awareness already exist in nature?" In such a case, we would say that biological systems have evolved to utilize this fundamental form of subtle-awareness in nature to produce simple but specific types of awareness in our brains. This is at the heart of understanding why the topology of V1 microcolumns might be so important and why we should focus our attention on their structure. The shape of the microcolumn generates a uniquely shaped EM field. QVA predicts that V1 microcircuits sculpt this natural form of subtle-awareness found in EM fields into discrete and unique instances of simple awareness known as qualia.

*What is the Role of Temporal Synchrony in Producing Visual Awareness?*

Temporal synchrony plays a dual role. The half-life of any given quale EM field is short. To effectively contribute to the visual experience, it is necessary to continually reactivate a microcircuit to refresh the electromagnetic field it produces. Moreover, by stimulating the appropriate microcircuits in synchrony, we are binding all the respective qualia into one coherent visual image in the same way the refresh rate of a computer screen restimulates pixels to create long-lasting images on your computer displays.

The thalamus is known to be highly connected throughout the cortex and is thought to play a central role in the production of consciousness. Moreover, support for the importance of the thalamus in consciousness is suggested by work using anesthetics with their targeted effect on the thalamus and the resultant loss of consciousness. Unlike some current theories that focus on the thalamus as the source of consciousness, QVA postulates the importance of the thalamus is based on its role of supporting temporal synchrony within the cortex.

The part of the thalamus that connects directly to V1 is the lateral geniculate nucleus (LGN). This connection serves as the dominant road by which visual information reaches the visual cortex. Moreover, thalomocortical circuits that connect the thalamus and V1 are well known to have a pacemaker like quality (Llinás and Ribary 2001). The reticular formation of the thalamus sends subthreshold EPSPs to V1 microcircuits and it is believed that reentrant communication from the higher visual centers (ex. V3, V4, V5) pushes these microcircuits past their threshold and initiates gamma synchrony for selected microcircuits (Escobar 2016). Thus, the thalamus has a pivotal role in establishing

temporal synchrony and is directly contributing to the process of binding individual qualia into our overall visual experience. Without this rhythmic, thalamic, subthreshold-priming (ex. in response to the application of anesthetics), the cerebral cortex continues to exhibit some neural activity but this activity cannot be bound into a coherent, conscious experience and the individual would appear, for all intents and purposes, unconscious.

## Conclusions

QVA postulates that, at least, the V1 microcolumns of several primates (macaques and humans for example), shape a fundamental form of awareness in electromagnetic fields through constructive and destructive interference.* This is highly dependent on the topology of the microcircuit itself and so the shape of the microcircuit will yield specific but simple forms of awareness like a point of red, green or blue.

The electromagnetic nature of these fields allows them to integrate themselves instantaneously into a larger field that contains other visual qualia. Together, these bits of awareness (arising from the millions of microcolumns in V1) produce our visual field.

The half-life of any given quale EM field is exceedingly short. Thus, a microcolumn can only significantly contribute to a visual experience through temporal synchrony since this allows each quale contribution to persist in the overall brain EM field. In addition, by producing these bits of awareness in a synchronous manner, we bind the individual qualia into a coherent experience in a manner similar to the refresh rate of a computer display.

Predictions that arise from this hypothesis are that we would expect repeating microcircuit structures since the same types of qualia would be found in a large proportion of the ocular dominance columns distributed throughout V1. Although there are millions of microcolumns in V1, there may only be 50-100 types since we can combine them to create an infinite number of possible visual representations. Currently, there is no cognitive or subjective experience theory that predicts repeating microcircuit structures in V1 of the occipital cortex.

ODCs correspond to individual points of the visual field and serve the purpose of being organizing centers for the 50-80 microcolumns they contain. This system would confer exquisite control of visual experiences to the visual cortex since any number of possible combinations of quale could be specified for each point of the visual field. Please review the example yellow vertical line described above.

In addition, to the predictions listed above, QVA also proposes that conserved (repeating) circuit structures should not be distributed randomly in V1. Distribution patterns should resemble the observed orientation-tuning pin wheel patterns (Crair et al. 1997) and location of blobs (Bartfeld and Grinvald 1992) observed in V1. A match between microcolumn-topology distribution patterns and these other listed patterns would support QVA since no such match is predicted by any other theory or model.

We have begun a rudimentary study of the structure of striate cortex in layers V and VI. The tools we have available at this time are simple but, through our simple approach, we have identified repeating clustering patterns in our target tissue. We realize this does not prove the QVA hypothesis but is only consistent with QVA. To truly establish QVA as a model that accurately describes the production of visual awareness it will be necessary to probe the structure of this region of the cortex with techniques that offer greater precision. We are hopeful that in the coming years the ability to describe the topology of neural circuits containing hundreds of neurons will become a common technology that can be used to answer some of the questions we raise here.

*Notes*

*A question can be raised about natural EM fields and their effect on the EM fields created by the brain. Transcranial magnetic stimulation (TMS) studies clearly show that brain EM fields can be disrupted by an external field with corresponding effects on conscious perception (Cowey and Walsh 2000, Overgaardet al. 2004). However, it is also clear that TMS generates fields with a much greater local amplitude than say the geomagnetic field of our planet. It is likely the cranium offers enough insulation to prevent significant alteration of brain EM fields since we do not normally experience the disruptions to conscious perception (the perception of phosphenes for example) that routinely occur when the visual cortex is stimulated with TMS.

## Aknowledgements

Part of the work in identifying cell cluster topologies was accomplished through the help of undergraduate students in the course Biology 410 (Perception and the Neural Correlates of Consciousness). Below is a list of the names of participating students listed alphabetically by last name: Sudeep Aditham, Evan Altschuler, Talah Bakdash, Triston Charlson, John Delgado, Ronnie Festok, Megan Jiang, Jordan Peyrot Des Gachons, Aditya Prakash, Priyadharshini Rathakrishnan, Sarah Romanelli, Jae Shim, Rishi Varan, Zhuoyang Ye, Teresa Zheng.

## References

Amunts K, Lepage C, Borgeat L, Mohlberg H, Dickscheid T, Rousseau MÉ et al. (2013) BigBrain: an ultrahigh-resolution 3D human brain model. *Science* 340(6139): 1472–1475.

Bartfeld E, Grinvald A (1992) Relationships between orientation-preference pinwheels, cytochrome oxidase blobs, and ocular-dominance columns in primate striate cortex. *Proceedings of the National Academy of Sciences USA* 89(24): 11905–11909.

Block N (1996) How can we find the neural correlate of consciousness? *Trends in Neurosciences* 19(11): 456–459.

Boehler C, Schoenfeld M, Heinze HJ, Hopf JM (2008) Rapid recurrent processing gates awareness in primary cortex. *Proceedings of the National Academy of Sciences* 105(25): 8742–8747.

Chalmers DJ (1995) Facing up to the problem of consciousness. *Journal of Consciousness Studies* 2(Jan): 200–219.

Cowey A, Walsh V (2000) Magnetically induced phosphenes in sighted, blind and blindsighted observers. *Neuroreport* 11(14): 3269–3273.

Crair MC, Ruthazer E, Gillespie D, Stryker M (1997) Ocular dominance peaks at pinwheel center singularities of the orientation map in cat visual cortex. *Journal of Neurophysiology* 77(6): 3381–3385.

Crick F, Koch C (2003) A Framework for Consciousness. *Nature Neuroscience* 6(2): 119–126.

Eckhorn R, Bauer R, Jordan W, Brosch M, Kruse W, Munk M et al. (1988) Coherent oscillations: a mechanism of feature linking in the visual cortex? Multiple electrode and correlation analyses in the cat. *Biological Cybernetics* 60(2): 121–130.

Eckhorn R, Frien A, Bauer R, Woelbern T, Kehr H (1993) High frequency (60-90 Hz) oscillations in primary visual cortex of awake monkey. *Neuroreport* 4(3): 243–246.

Eckhorn R (1994) Oscillatory and non-oscillatory synchronizations in the visual cortex and their possible roles in associations of visual features. *Progress in Brain Research* 102(Mar): 405–426.

Escobar WA (2013) Quantized Visual Awareness. *Frontiers in Psychology* 4(Nov): 1–11.

Escobar A (2016) QVA: A massively parallel model for vision. *Psychology of Consciousness: Theory, Research, and Practice* 3(3): 222–238.

Fries P, Roelfsema PR, Engel AK, König P, Singer W (1997) Synchronization of oscillatory responses in visual cortex correlates with perception in interocular rivalry. *Proceedings of the National Academy of Sciences USA* 94(23): 12699–12704.

Hubel D, Wiesel T (1974) Sequence Regularity and Geometry of Orientation Columns in the Monkey Striate Cortex. *Journal of Comparative Neurology* 158(3): 267–294.

Hubel D, Wiesel TN, Stryker M (1978) Anatomical demonstration of orientation columns in macaque monkey. *The Journal of Comparative Neurology* 177(3): 361–379.

John E (2002) The neurophysics of consciousness. *Brain Research Reviews* 39(1): 1–28.

Keliris GA, Logothetis NK, Tolias AS (2010) The role of the primary visual cortex in perceptual suppression of salient visual stimuli. *The Journal of Neuroscience* 30(37): 12353–12365.

Kosslyn SM, Ganis G, Thompson WL (2001) Neural Foundations of Imagery. *Nature Reviews | Neuroscience* 2(9): 635–642.

Kreiter AK, Singer W (1996) Stimulus-dependent synchronization of neuronal responses in the visual cortex of the awake macaque monkey. *The Journal of Neuroscience* 16(7): 2381–2396.

Lamme VA (2003) Why visual attention and awareness are different. *Trends in Cobnitive Sciences* 7(1): 12–18.

Leopold D, Logothetis N (1996) Activity-changes in early visual cortex reflect monkeys' percepts during binocular rivalry. *Nature* 379(Feb): 549–553.

Llinás R, Ribary U (2001) Consciousness and the brain: the thalamocortical dialogue in health and disease. *Annals of the New York Academy of Sciences* 929(Apr): 166–175.

Mazzi C, Mancini F, Savazzi S (2014) Can IPS reach visual awareness without V1? Evidence from TMS in healthy subjects and hemianopic patients. *Neurophysiologia* 64(Nov): 134–144.

McFadden J (2002a) Synchronous firing and its influence on the brain's electromagnetic field. *Journal of Consciousness Studies* 9(4): 23–50.

McFadden J (2002b) The conscious electromagnetic information (cemi) field theory: the hard problem made easy? *Journal of Consciousness Studies* 9(8): 45–60.
McFadden J (2013) CEMI field theory: closing the loop. *Journal of Consciousness Studies* 20(1-2): 153–168.
Mehta AU (2000) Intermodal selective attention in monkeys I: distribution and timing across visual areas. *Cerebral Cortex* 10(4): 343–358.
Mountcastle V (2003) Introduction. *Cerebral Cortex* 13(1): 2–4.
Muralidhar S, Wang Y, Markram H (2014) Synaptic and cellular organization of layer 1 of the developing rat somatosensory cortex. *Frontiers in Neuroanatomy* 7(Article 52): 1–17
Overgaard M, Nielsen J, Fuglsang-Fredricksen A (2004) A TMS study of the ventral projections from V1 with implications for the finding of neural correlates of consciousness. *Brain and Cognition* 54(1): 58–64.
Pascual-Leone A, Walsh V (2001) Fast backprojections from the motion to the primary visual area necessary for visual awareness. *Science* 292(5516): 510–512.
Peters A, Sethares C (1991) Organization of pyramidal neurons in area 17 of monkey visual cortex. *The Journal of Comparative Neurobiology* 306(1): 1–23.
Peters A, Walsh M (1972) A Study of the organization of apical dendrites in the somatic sensory cortex of the rat. *Journal of Comparative Neurology* 144(3): 253–268.
Pockett S, Bold GEJ, Freeman WJ (2009) EEG synchrony during a perceptual-cognitive task: widespread phase synchrony at all frequencies. *Clinical Neurophysiology* 120(4): 695–708.
Singer W (1998) Consciousness and the structure of neuronal representations. *Philosophical Transactions of the Royal Society London B Biological Science* 353(1377): 1829–1840.
Silvanto J, Lavie N, Walsh V (2005) Double Dissociation of V1 and V5/MT activity in visual awareness. *Cerebral Cortex* 15(11): 1736–1741.
Tong F (2003) Primary visual cortex and visual awareness. *Nature Reviews Neuroscience* 4(Mar): 219–229.
Tononi G (2008) Consciousness as integrated information: a provisional manifesto. *Biological Bulletin* 215(3): 216–242.
Tononi G, Koch C (2008) The neural correlates of consciousness. *Annals of the New York Academy of Sciences* 1124(1): 239–261.
Von Bonin G, Mehler W (1971) On columnar arrangement of nerve cells in cerebral cortex. *Brain Research* 27(1): 1–9.
Witzel C, Gegenfurtner KR (2018) Color perception: objects, constancy, and categories. *Annual Review of Vision Science* 4(Sep): 475–499.
Yu TL, Zeki S (2014) Perceptual asynchrony for motion. *Frontiers in Human Neuroscience* 8(Mar): 108.
Zeki S (2015a) Area V5—a microcosm of the visual brain. *Frontiers in Integrative Neuroscience* 9(21).
Zeki S (2015b) Review article: a massively asynchronous, parallel brain. *Philosophical Transactions of the Royal Society B: Biological Science* 370(1668).
Zeki S, Bartels A (1999) Toward a theory of visual consciousness. *Consciousness and Cognition* 8(2): 225–259.

*Athens Journal of Sciences- Volume 7, Issue 3, September 2020 – Pages 143-158*

# Intuitionism and Computer Science – Why Computer Scientists do not Like the Axiom of Choice

*By Thomas Fehlmann[*] & Eberhard Kranich[±]*

*The Axiom of Choice (AC) says that every set has a representative element. However, deterministic computers cannot produce arbitrary elements. They need some algorithm that tells them, which one to choose. But then, the element is no longer arbitrary. Even for a true random generator, you will need entropy. This is data gathered from outside the system, and we as Theoretical Computer scientists do not like that. Thus, we need to understand the Axiom of Choice better. For this, we use a model of Combinatory Logic.*

**Keywords:** *Combinatory logic, combinatory algebra, intuitionism, axiom of choice, computability, software testing, artificial intelligence*

## Introduction

Zermelo–Fraenkel (ZF) set theory, named after mathematicians Ernst Zermelo and Abraham Fraenkel, is an axiomatic system that was proposed in the early twentieth century to formulate a theory of sets free of paradoxes such as Russell's paradox. For an introduction, see e.g., Potter (2004).

The famous *Banach–Tarski paradox* is a theorem in set-theoretic geometry, which states the following: Given a solid sphere in 3-dimensional space, there exists a decomposition of the sphere into a finite number of disjoint subsets, which can then be put back together in a different way to yield two identical copies of the original sphere. Indeed, the reassembly process involves only moving the pieces around and rotating them without changing their shape (Banach and Tarski 1924).

The number of pieces was subsequently reduced to five by Robinson (1947), although the pieces are extremely complicated. Five pieces are minimal, although four pieces are enough if the single point at the center is neglected.

This sounds strange, counter-intuitive, and impracticable. Nevertheless, it relies on the following reasoning:

If the Axiom of Choice (AC) holds, then non-measurable sets exist (Tao 2011).

If non-measurable sets exist, the Banach-Tarski paradox holds (Pawlikowski 1991).

A set is called *measurable*, if there is a systematic way to assign a number to each suitable subset, a *Size*, such that sizes of subsets can be added to get a measure for the size of the original set. For details, see Potter (2004).

[*]Senior Researcher, Euro Project Office AG, Switzerland.
[±]Senior Researcher, Euro Project Office AG, Switzerland.

So, why can the Banach-Tarski paradox be proven to be true, logically? Is mathematical logic flawed? No: A formal proof of the paradox uses an infinity of spheres (set of all points whose distance to origin is constant), excluding the spheres of radius 0. For an elegant proof, see Rauglaudre (2017). For a quick idea instead of a full proof, just imagine that you always can fill your sphere with infinitely many copies of that sphere, pick a point in each sphere, rotate them by an angle to get yet another new sphere but different from all previously picked spheres – this argument uses the AC! – and still get infinitely many copies. Now separate the original set of spheres from the copies and you have two different, identical spheres.

## The Axiom of Choice and its Variants

The Axiom of Choice (AC) says that given any family of non-empty sets $S_i$ for $i \in I$, there exists a function such that $f(i) \in S_i$ for all $i \in I$. $f$ is called a *Choice Function.*

Obviously, the Banach-Tarski paradox makes it difficult to believe that the AC is indispensable in mathematics. Equivalent to the AC is the *Well-ordering Theorem.* It states that every set can be well-ordered. A set $X$ is well-ordered by a strict total order if every non-empty subset of $X$ has a least element under the ordering. This is intuitively not compelling, too.

### *Real, Irrational Numbers Require the AC*

However, the AC is indispensable for many important – and intuitive – mathematical results; among them

- Let $\mathbb{R}$ be the closure of $\mathbb{Q}$, the set of all rational numbers under convergent sequences. Then, the convergence point is also in $\mathbb{R}$.
- Many square numbers, such as $\sqrt{2}$, are not rational numbers, since assuming there are natural numbers $p, q \in \mathbb{N}$ with $\sqrt{2} = p/q$ leads to the conclusion that both $p, q$ must be dividable by $2$. This contradicts the possibility of representing rational numbers by co-primes[1].

Nevertheless, irrational numbers are unhandy for a digital device. You only can represent them by their properties, i.e., as symbols.

*Combinatory Logic* is a notation to eliminate the need for quantified variables in mathematical logic. The issue addressed with combinatory logic is the AC. What means "there exists something", $\exists x \in M$, in some set $M$? Informally, the AC says that given any collection of non-empty sets, it is possible to select exactly one object from each set, without requiring an algorithm saying how the selection

[1]Co-primes are numbers which have $1$ as the greatest common denominator.

is done. In the theory of *Complex Analysis*, such an algorithm seems an unnecessary condition; in fact, complex analysis proved to be very successful without requiring constructive selection algorithms.

*The Intuitionistic Variant of the Axiom of Choice*

In Computer Science, the existence of selection algorithms seems a natural condition for the applicability of the AC. On a computer, nothing exists resembling a program or process without an algorithm that effectively constructs it.

Thus, as computer scientists we always presume a stronger version of the AC: there exists means, there exists an algorithm that allows to select exactly one representative from each collection of sets.

Interestingly, this conditioning of the AC to Mathematical Logic has wide consequences. For instance, there exists a countable model of the real numbers, meeting all the axioms for real numbers. We can assure that the limit of any convergent sequence of real numbers exists and that it is itself a real number by selecting the convergence sequences themselves as a model. This is a measurable and enumerable set. In fact, there is no other way on a computer to implement real numbers than by such sequences.

The famous digital representation for the relation between diameter and circumference of a circle, $\pi$, is an infinite sequence of digits that never repeat themselves; thus, not anything that exists within a digital device, not even within the universe. Only sequences that converge towards $\pi$ do exist.

However, the Banach–Tarski paradox does not hold with the intuitionistic version of the AC, since there is no way selecting the right rotated spheres that allow to split the original ball into two identical spheres.

## Combinatory Logic

There is a mathematical theory about *Combinatory Algebras* (Engeler 1995) that explains quite generally how to combine topics in areas of knowledge. Combination is not only on the basic level possible; you can also explain how to combine topics on the second level; sometimes called meta-level. Intuitively, we would expect such a meta-level describing knowledge about how to deal with different knowledge areas.

Combinatory algebras are models of *Combinatory Logic* (Curry and Feys 1958, Curry et al. 1972). These are algebras that are combinatory complete; i.e., there is a combination operation $M \bullet N$ for all elements $M, N$ in the combinatory algebra and the following two *Combinators* $\mathbf{S}$ and $\mathbf{K}$ can be defined with the following properties

$$\mathbf{K} \bullet M \bullet N = M \tag{1}$$

and

$$\mathbf{S} \bullet M \bullet N \bullet L = M \bullet L \bullet (N \bullet L) \tag{2}$$

where $M, N, L$ are elements in the combinatory algebra.

Thus, the combinator **K** acts as projection, and **S** is a substitution operator for terms in the combinatory algebra. Like an assembly language, the **S**-**K** terms become quite lengthy and are barely readable by humans, but they work fine as a foundation for computer science.

The power of these two operators is best understood when we use them to define other, handier, and more understandable combinators:

*Identity*

The identity combinator is defined as

$$\mathbf{I} \coloneqq \mathbf{S} \bullet \mathbf{K} \bullet \mathbf{K} \tag{3}$$

Indeed, $\mathbf{I} \bullet M = \mathbf{S} \bullet \mathbf{K} \bullet \mathbf{K} \bullet M = \mathbf{K} \bullet M \bullet (\mathbf{K} \bullet M) = M$. Association is to the left.

*Functionality by the Lambda Combinator*

Curry's *Lambda Calculus* (Barendregt 1977) is a formal language that can be understood as a prototype programming language.

The algebra of **S**-**K** terms models the lambda calculus by recursively defining the *Lambda Combinator* for a variable **x** as follows:

$$\begin{gathered} \mathbf{L_x} \bullet x = \mathbf{I} \\ \mathbf{L_x} \bullet Y = \mathbf{K} \bullet Y \text{ if } Y \text{ different from } \mathbf{x} \\ \mathbf{L_x} \bullet M \bullet N = \mathbf{S} \bullet \mathbf{L_x} \bullet M \bullet \mathbf{L_x} \bullet N \end{gathered} \tag{4}$$

The definition holds for any variable **x** in the combinatory algebra.

For more details about the foundations of Mathematical Logic, see for instance Barwise (1977) or Potter (2004). For more combinators in combinatory logic, see e.g., Zachos (1978).

## Arrow Terms

Let $\mathcal{L}$ be the set of all assertions over a given domain. Examples include statements about customer's needs, solution characteristics, methods used, program states, test conditions, etc. These statements are assertions about the business domain we are dealing with.

An *Arrow Term* is recursively defined as follows:

Every element of $\mathcal{L}$ is an arrow term

Let $a_1, \ldots, a_m, b$ be arrow terms. Then

$$\{a_1, \ldots, a_m\} \to b \tag{5}$$

is also an arrow term.

The left-hand side of an arrow term is a finite set of arrow terms and the right-hand side is a single arrow term. This definition is recursive. The arrows might suggest cause-effect, not logical imply.

*The Algebra of Arrow Terms*

Denote by $\mathcal{G}(\mathcal{L})$ the power set containing all *Arrow Terms* of the form (5). The formal, recursive, definition, in set-theoretical language, is given in equation (6):

$$\begin{gathered}\mathcal{G}_0(\mathcal{L}) = \mathcal{L} \\ \mathcal{G}_{n+1}(\mathcal{L}) = \\ \mathcal{G}_n(\mathcal{L}) \cup \left\{\{a_1, \dots, a_m\} \to b \middle| a_1, \dots, a_m, b \in G_n(L), m \in \mathbb{N}\right\}\end{gathered} \tag{6}$$

for $n = 0, 1, 2, \dots$ $\mathcal{G}(\mathcal{L})$ is the set of all (finite and infinite) subsets of the union of all $\mathcal{G}_n(\mathcal{L})$:

$$\mathcal{G}(\mathcal{L}) = \bigcup_{n \in \mathbb{N}} \mathcal{G}_n(\mathcal{L}) \tag{7}$$

The elements of $\mathcal{G}_n(\mathcal{L})$ are arrow terms of level $n$. Terms of level $0$ are *Assertions*, terms of level $1$ *Rules*. A set of rules is called *Rule Set* (Fehlmann 2016). In general, a rule set is a finite set of arrow terms. We call infinite rule sets a *Knowledge Base*. Hence, knowledge is a potentially unlimited set of rules sets containing rules about assertions regarding our domain.

*Combining Rule Sets*

We can combine two rule sets as follows:

$$M \bullet N = \{c | \exists \{b_1, b_2, \dots, b_m\} \to c \in M;\ b_i \in N\} \tag{8}$$

*Arrow Term Notation*

To avoid the many set-theoretical parenthesis, the following notations are applied:

$a_i$ for a finite set of arrow terms, $i$ denoting some finite indexing function for arrow terms.
$a_1$ for a singleton set of arrow terms; i.e. $a_1 = \{a\}$ where $a$ is an arrow term.
$\emptyset$ for the empty set, such as in the arrow term $\emptyset \to a$.
$(a)$ for a potentially infinite set of arrow terms, where $a$ is an arrow term.

The indexing function cascades, thus $a_{i,j}$ denotes the union of a finite number of $m$ arrow term sets

$$a_{i,j} = a_{i,1} \cup a_{i,2} \cup \ldots \cup a_{i,j} \cup \ldots \cup a_{i,m} = \bigcup_{k=1}^{m} a_{i,k} \tag{9}$$

In terms of these conventions, $(x_i \to y)_j$ denotes a rule set, i.e., a non-empty finite set of arrow terms, each having at least one arrow. Thus, such set has level 1 or higher.

With this notation, the application rule for $M$ and $N$ now reads

$$M \bullet N = \big((b_i \to a) \bullet (b_i)\big) = \{a | \exists b_i \to a \in M;\ b_i \subset N\} \tag{10}$$

*Arrow Terms – A Model of Combinatory Logic*

The algebra of arrow terms is a combinatory algebra and thus a model of combinatory logic.

The following definitions demonstrate how arrow terms implement the combinators **S** and **K** fulfilling equations (1) and (2).

$\mathbf{I} = (a_1 \to a)$ is the *Identification*; i.e. $(a_1 \to a) \bullet (b) = (b)$

$\mathbf{K} = (a_1 \to \emptyset \to a)$ selects the 1st argument:

$\mathbf{K} \bullet (b) \bullet (c) = \big((b_1 \to \emptyset \to b) \bullet (b)\big) \bullet (c) = (\emptyset \to b) \bullet (c) = (b)$

$\mathbf{KI} = (\emptyset \to a_1 \to a)$ selects the 2nd argument:

$\mathbf{KI} \bullet (b) \bullet (c) = \big((\emptyset \to c_1 \to c) \bullet (b)\big) \bullet (c) = (c_1 \to c) \bullet (c) = (c)$

$\mathbf{S} = \Big(a_i \to \big(b_j \to c\big)\Big)_1 \to \Big((d_k \to b)_i \to \big(b_{j,i} \to c\big)\Big)$

Therefore, the algebra of arrow terms is a model of combinatory logic.

The proof that the arrow terms' definition of **S** fulfils equation (2) is somewhat more complex. The interested reader can find it in Engeler (1981). With **S** and **K,** an abstraction operator can be constructed that builds new knowledge bases. This is the *Lambda Theorem*; it is proved along the same way as Barendregt's Lambda combinatory (Barendregt 1977, Fehlmann 1981).

## Neural Algebra

Engeler uses the arrow terms for a brain model (Engeler 2019). A directed graph, together with a firing law at all its nodes, constitute the connective basis of the brain model. The model itself is built on this basis by identifying brain functions with parts of the firing history. Its elements may be visualized as a directed graph, whose nodes indicate the firing of a neuron. *Cascades* describe firing between nodes (neurons) and is represented by arrow terms

$\{a_1, \ldots, a_m\} \to b$ where $a_1, \ldots, a_m$ are sub-cascades, while the right sub-cascade $b$ describes the characteristic leave of its firing history graph. The Neural Algebra is defined as a collection of subsets of the set of cascades. With the application rule (10), we have an algebraic structure.

Within this setting, it is possible to define models for reasoning and problem solving. However, not only flat reasoning, also the control operations. This is represented as a solution $X$ for the control problem $\boldsymbol{C} \bullet X = X$, where $\boldsymbol{C}$ is the *Controlling Operator*. Engeler presents in an elegant way combinators that represent basic operations of the brain, e.g., problem solving, or balancing on a bike.

Discrimination between choices, and self-reflection about how to take decisions, how to address problems, as well as learning and comprehending can also be modeled with that approach.

Since the number of cascades that a brain can produce is finite and limited – by the lifespan of the brain – solution to the fixpoint control problems turn out to be finite cascades. It is tempting to identify cascades with though processes.

## The Algebra of Test Cases

Test cases are a mapping of arrow terms onto data movement maps, see below. The data movements induce a sizing valuation on this algebra by counting the number of data movements executed once per test case. We rely on the ISO standard 19761 COSMIC (ISO/IEC 19761 2011).

### *Data Movement Maps*

*Data Movement Maps* are a way to model a piece of software by connecting objects of interest, representing functionality, persistent stores, devices, and other applications, based on the COSMIC standard. The connectors represent *Data Movements*. They have some resemblance to *UML Sequence Diagrams* but with less detail; thus, without guards, loops, and alternative fragments (Bell 2004). Also, sequencing is not prescribed.

Every data movement moves a *Data Group*, which can be thought as a data record moving information from one object of interest to another. Usually, its uniqueness is indicated by color-filled trapezes (Figure 1). Another move of same data group between the same objects within a functional process lets the trapeze blank. The number of unique movements is called *Functional Size* according COSMIC and denoted by $\|\mathfrak{s}\|$, for any data movement map $\mathfrak{s} \in \mathfrak{S}$ where $\mathfrak{S}$ is a set of data movement maps (COSMIC Measurement Practices Committee 2017).

**Figure 1.** *Sample Data Movement Map*

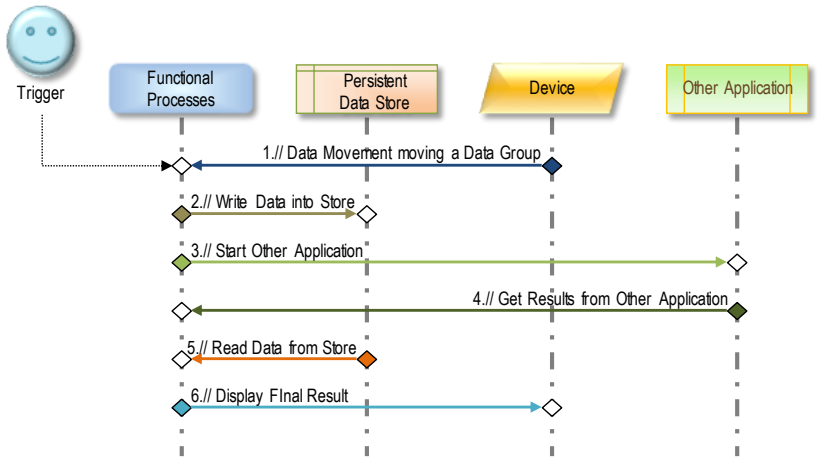


Data movement maps are explained in Fehlmann (2020) and in more detail in Fehlmann (2016).

*The Combinatory Algebra of Test Cases*

Arrow terms over the language of test assertions, or program states, represent test cases in a straightforward way. In formula (5), the left-hand side of the arrow term $\{a_1, \dots, a_m\} \to b$ represents test data $a_1, \dots, a_m$ as a sequence of program states, while the right-hand side $b$ is the expected resulting program state after executing the test case. Let $\mathfrak{S}$ be a finite set of data movement maps. A test case $\{a_1, \dots, a_m\} \to b$ can be *executed* in $\mathfrak{S}$ if a data movement map in $\mathfrak{S}$ exists that transforms the program states $a_1, \dots, a_m$ into $b$.

Denote by $\bigcup \mathfrak{S}$ the union of all data movement maps in $\mathfrak{S}$. The *union* is defined in the straightforward manner by identifying all identical objects of interest within all data movement maps in $\mathfrak{S}$. Obviously, $\bigcup \mathfrak{S}$ is itself a data movement map. It represents the program under test, or more exactly, the part of the program that is covered by test cases, executable in $\mathfrak{S}$. Note that when combining executable test cases from program $\bigcup \mathfrak{S}$ using equation (10), the result is also executable in $\bigcup \mathfrak{S}$.

*Test Automation*

The arrow terms serve primarily as a grammar for test cases, but the properties of a combinatory algebra allow for much more. Test can be combined, using equation (8) or any other combinator. This allows to generate as many test cases as we want and need for achieving full test coverage.

Therefore, it is no longer an excuse for not testing large and complex systems that the scarcity of resources, especially proficient software testers, do not allow for a full test, testing all of the software even for large systems such as today's

trainsets, or *Advanced Driving Assistance Systems* (ADAS), or autonomous vehicles, in case they ever will hit our roads.

It is noteworthy that programmers who want to set up test concatenation $M \bullet N$ for automatic testing, need access to the test cases in $N$ that provide the responses needed for $M$. Otherwise, combining tests is unsafe or cannot be automated. The equation (8) does exactly this, providing the existence of an arrow term means that a rule is available that tells the programmer, which test case to take. In other words, combination of tests also traces the history how these tests have emerged. This allows to validate combined tests.

This interpretation of the logical existence means that we apply here the intuitionistic variant of the axiom of choice. Programmers, and even more: testers, would reject combining tests with equation (8) unless we silently apply the intuitionistic, stronger form of the AC.

*Keeping the Number of Generated Test Cases Low*

However, a testing environment that produces test cases without end is not very practical either. It is therefore necessary to have a selection algorithm that allows to direct the test case generator towards the relevant tests.

This can be achieved by means of *Transfer Functions*, which are in detail explained in Fehlmann (2016) – that map the selection of test cases back onto customer values.

In this paper the so-called linear multiple-response transfer functions are of special interest. Such transfer functions are defined by equations of the form

$$\boldsymbol{y} = \boldsymbol{A}\boldsymbol{x} \tag{11}$$

where $\boldsymbol{y}$ is the predefined goal profile, $\boldsymbol{A}$ as transfer function is a matrix and hence a linear transfer function which measures the effects of test cases in view of the user stories that represent the customer's needs and values. $\boldsymbol{x}$ is the vector which describes the yet to be determined, initially unknown, importance of the test cases. Clearly, $\boldsymbol{x}$ depends on the matrix $\boldsymbol{A}$ and the goal profile $\boldsymbol{y}$

However, since test cases are what we are looking for, the function $\boldsymbol{A}$ is not given, either. It depends on the test cases – preexisting and generated – that we use in our test suite. In practice, we start with a rule set – *Test Cases* – that can be grouped in *Test Stories* and extended as needed; see Fehlmann (2020). Test stories and *User Stories* allow representing the function $\boldsymbol{A}$ as a matrix. The user stories represent the requirements, based on customer needs.

**Figure 2.** *Equation* $\boldsymbol{y} = \boldsymbol{Ax}$ *as a Matrix between User Stories and Test Stories*

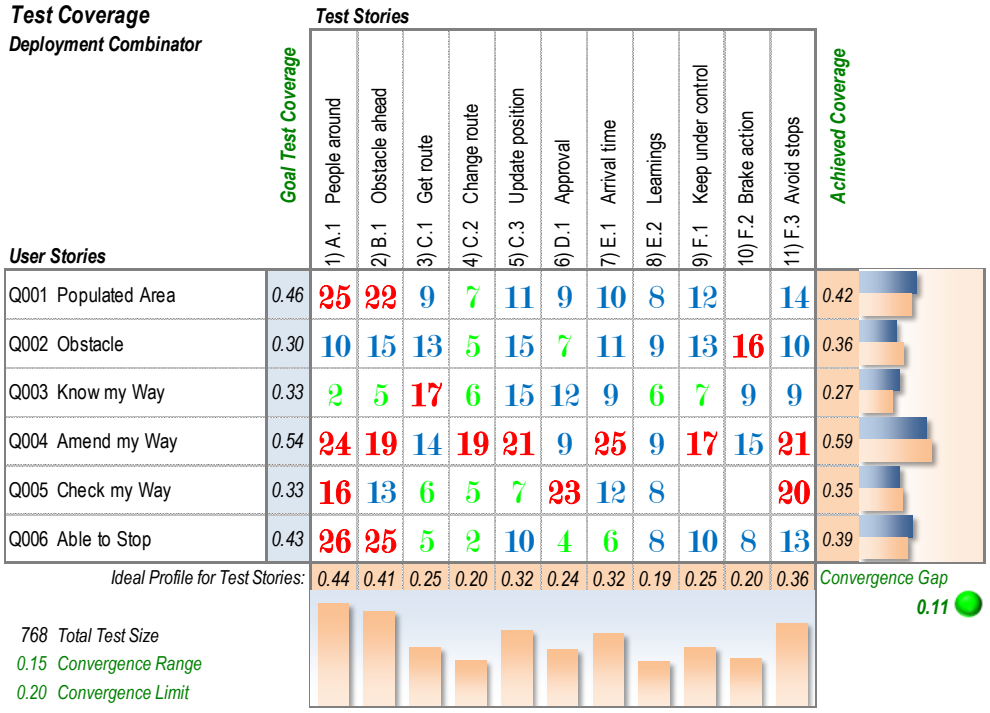


The goal vector $\boldsymbol{y}$ is labelled *Goal Test Coverage* in Figure 2; the *Achieved Result* is the product of matrix $\boldsymbol{A}$ and vector $\boldsymbol{x}$, at the bottom of the matrix. The vector $\boldsymbol{x}$ is widely unknown at the time when tests are designed. Not even its dimension – the number of tests – is obvious, nor the topics that merit being tested. Thus, there are many ways of designing a valid test strategy; however, the convergence gap (see equation (14) below) must remain small.

*What Number to Put into the Matrix Cells?*

The number in the matrix cells represent the total test size that correlated between the respective user story and test story. This *Cell Test Size* is the number of data movements within all test cases in the specific Test Story that pertain to the respective user story. The main problem is how to find a vector $\boldsymbol{y}$ representing qualitative or quantitative user needs, as a profile. A profile is a vector in some space of user needs with Euclidian length $= 1$. Agile teams have a process to prioritize user stories; however, they usually do not care about representing priorities as a profile vector.

Finding $\boldsymbol{A}$ and $\boldsymbol{x}$ in equation (11) is not trivial. However, in practice, the even bigger problem is that the goal vector $\boldsymbol{y}$ is often unknown. The needs of the customer, or user, in view of testing are nothing that development teams know automatically, because it involves safety, privacy and security in addition to functionality. We need a profile for all explicit and implicit requirements.

Formally, the cell numbers are constructed as follows:

Test stories are a collection of rule sets (test cases) that share a common purpose. Let $\boldsymbol{t} \in \boldsymbol{S}$ be a test story, member of some rule set $\boldsymbol{S}$.

For every test story $\boldsymbol{t}$, there is a mapping

$$\boldsymbol{map}(\boldsymbol{t}) \in \bigcup \mathfrak{S} \tag{12}$$

where $\bigcup \mathfrak{S}$ is the set of all data movement maps within a software program, as before.

Furthermore, there is a choice function $\|\boldsymbol{map}(\boldsymbol{t})\|_{\boldsymbol{f}}$ identifying which data movements pertain to some specific user story $\boldsymbol{f}$ and counting them.

For each cell, we start with a rule set of test cases $\boldsymbol{t}_{i,j} \in \boldsymbol{S}_j$, where $i, j$ are the respective cell indices of the matrix $\boldsymbol{A}$ and $\boldsymbol{S}_j$ is the respective test story in that matrix. then

$$\sum \|\boldsymbol{map}(\boldsymbol{t}_{i,j})\|_{\boldsymbol{f}} \tag{13}$$

counts for each test case how many data movements pertain to the respective user story. The summation runs over all test cases $\boldsymbol{t}_{i,j} \in \boldsymbol{S}_j$ for each matrix cell with index $i, j$.

A data movement may appear in many test cases and pertain to more than a single user story. We count the total amount of times that a data movement is used, not the data movements as for test size.

*Finding the Optimum Test Cases to be Generated*

There exists a family of methods – the *Analytic Hierarchy Process* (AHP) and *Quality Function Deployment* (QFD), explained in the series of international standards 16355 (ISO 16355-1:2015 2015) that allow to derive such profile vectors in a professional and repeatable manner (Saaty 2003). Examples are available in Fehlmann (2020).

The idea is simple: if we can focus on test cases that pertain to customer needs, we have an instrument that helps us selecting those test cases that best extend testing towards a full coverage of everything that has value for the customer. Thus, we must define a choice function that achieves this.

Fehlmann and Kranich (2020) have tried to find such a choice function, using algebraic methods to define a sensitivity analysis procedure for any linear matrix with Eigenvector solutions, such as in QFD. However, the problem is complex, and possibly unsolvable. There may be approximation methods that can be used in practice.

The goal is to find a vector $\boldsymbol{x}$ and a matrix $\boldsymbol{A}$ such that

$$\|\boldsymbol{y} - \boldsymbol{A}\boldsymbol{x}\| < \boldsymbol{\varepsilon} \tag{14}$$

where $\|...\|$ denotes the Euclidean norm for vectors, called the *Convergence Gap*, and $\boldsymbol{\varepsilon}$ is the upper limit for an acceptable convergence gap. This has to do with the axiom of choice AC for the existence of real, irregular numbers in $\mathbb{R}$. Finding vector $\boldsymbol{x}$ and a matrix $\boldsymbol{A}$ is an iterative process. Finding test cases becomes equivalent to proving that a certain sequence of real numbers converges. Thus, testing is a model of combinatorial algebra.

Using the combination rule (10), it is possible to generate the set of all sensible test cases. Together with the convergence gap as a metric, or hash function, the formula (14) allows to select those test cases that are relevant, and therefore limit the growth rate for newly generated test cases.

## The Internet of Things (IoT) as a Simple Model

Since translating the theoretical background in practice is probably not so easy, we mention a short, simple example from IoT. The problem of generating new test cases is made considerably easier by assuming that adding another IoT "thing" adds more data movements that need to be included in tests. The example is a simple search app that looks for items in a database (Figure 3).

**Figure 3.** *Simple Search App*

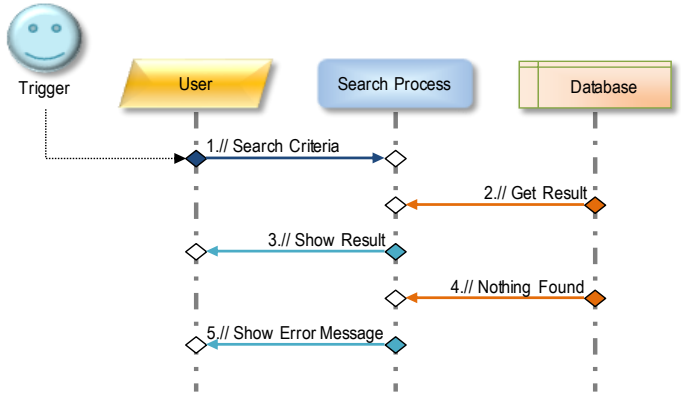


The functional size of this app is the number of data movements between objects of interest, according to COSMIC (COSMIC Measurement Practices Committee 2017). Now we add IoT devices – e.g., a sensor and an actuator that interact with the environment (Figure 4).

**Figure 4.** *IoT Search Concert App*

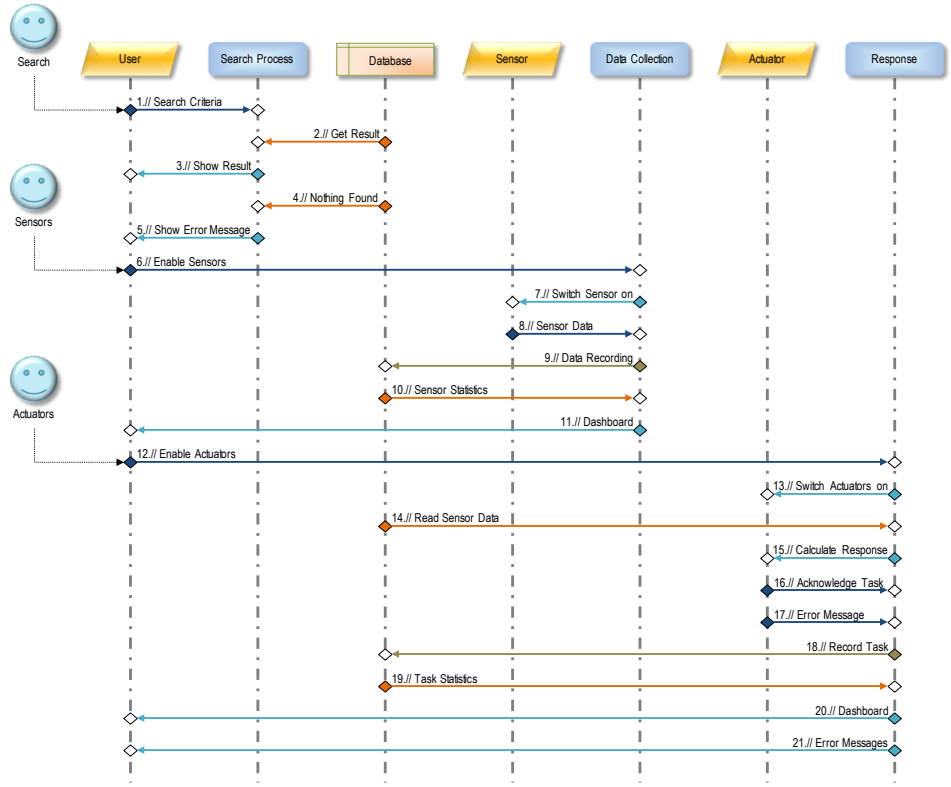


The IoT search concert still focuses on search, despite the additional functionalities. Thus, user needs for the two programs are identical. Consequently, the user stories are similar, although the user story priority profiles differ (Figures 5-6).

**Figure 5.** *User Stories for Simple Search*

| | User Stories Topics | As a ... | I want to ... | such that ... | so that ... | Priority Weight | Priority Profile |
|---|---|---|---|---|---|---|---|
| 1) | Q001 Search Data | *Search Data App User* | *find data matching my search criteria* | *It's attractive* | *I know when data exists* | *32%* | *0.55* |
| 2) | Q002 Answer Questions | *Search Data App User* | *know whether some data exists* | *answers are correct* | *I know when data doesn't exist* | *40%* | *0.68* |
| 3) | Q003 Keep Data Safe | *Search Data App User* | *make sure my data is safe* | *it cannot be deleted* | *I can retrieve it if necessary* | *29%* | *0.49* |

**Figure 6.** *User Stories for IoT Search Concert*

| | User Stories Topics | As a ... | I want to ... | such that ... | so that ... | Priority Weight | Priority Profile |
|---|---|---|---|---|---|---|---|
| 1) | Q001 Search Data | *IoT Data App User* | *find data matching my sensor data or search string* | *I can use it* | *I know when data exists* | *28%* | *0.49* |
| 2) | Q002 Answer Questions | *IoT Data App User* | *know whether some data or explanation exists exists* | *I can create it* | *I know when data doesn't exist* | *37%* | *0.64* |
| 3) | Q003 Keep Data Safe | *IoT Data App User* | *make sure my data is safe and repeatable* | *I can use actuators to protect items* | *I can retrieve it if necessary* | *35%* | *0.60* |

As before, the choice functions $\|map(t)\|_f$ define which data movements pertain to which user story. This allows constructing test coverage matrices for both, the Simple Search, and the IoT Search Concert. The test stories remain the same for both apps; the test cases for Simple Search also apply for IoT Search Concert.

The IoT Search Concert needs considerably more test cases, to cover additional sensor and actuator functionality. The growth in test size (= total number

of data movements in test cases according to COSMIC, see above) is considerably. Test size increases from 46 to 235.

These test cases can easily be constructed by concatenating unit tests for the IoT devices with the test cases already in place for the Simple Search App, using equation (10).

Obviously, the number of possible combinations grows exponentially and would soon exceed all available test capacity. This growth can be kept under control by selecting only those new test cases that keep the convergence gap of the test coverage matrix small enough, solving $\boldsymbol{y} = \boldsymbol{Ax}$ (Figures 7-8).

**Figure 7.** *Simple Search Test Coverage*

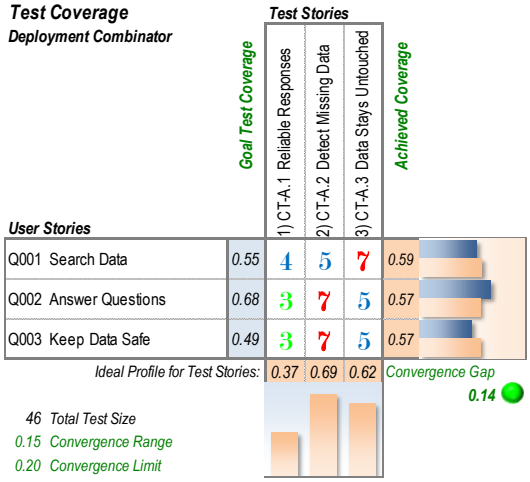


**Figure 8.** *IoT Search Test Coverage*

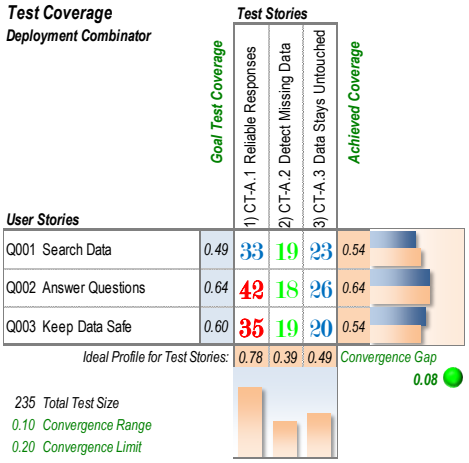


For *Artificial Intelligence* (AI), such search algorithms are typical methods. Using the convergence gap as a hash function for selecting meaningful test cases limits the growth of the search tree for test cases. For more details, see Fehlmann (2020).

## The Axiom of Choice and Artificial Intelligence

The misconception about computability of non-measurable structures – such as real numbers $\mathbb{R}$ – is also responsible for a very actual problem: some people believe that AI can solve problems; however, AI always approximates solving a problem. If AI comes without anything resembling the convergence gap it is most probably useless. You cannot rely on AI decisions without measuring accuracy.

Nevertheless, testing AI is possible, and not too difficult (Fehlmann and Kranich 2019). However, it cannot test the neuronal network – e.g., the *Support Vector Machine* (Gunn 1998) – itself but only its behavior in certain test situations. This is also explaining intuitively why testing never can prove anything. Testing software is always an approximation by a finite number of test cases, be it AI or traditional algorithmic programming. We always need a constructive choice function that selects relevant test cases for the approximation.

This suggests also that testing without a convergence gap is deceptive and potentially misleading.

Testing AI is done by construction of data movement maps that describe the expected behavior (Fehlmann and Kranich 2019). These data movement maps do not represent the program code; rather the behavior expected by the user.

The choice function selecting relevant test cases is therefore relevant. It is all but obvious which to choose, but it makes testing AI a matter of understanding its expectations in an intelligent machine. To believe that AI is intelligent by itself is like believing that the Banach-Tarski sphere can be split into two.

## Open Questions

Besides sensitivity analysis for matrices, there is one very stringent question open: can we define combinators that help us in generating meaningful additional tests? Like what Engeler did for neural networks?

Furthermore, is there a connection between sensitivity analysis and such combinators? Both questions may not only lead to practical solutions, but also interesting theoretical insight in the role of the axiom of choice for software engineering.

## Conclusions

Computer science uses choice functions only in a constructive way; existence of a choice always means existence of an algorithm that does the choice. This is counter-intuitive to human perception of the world but reflect the standpoint of mathematical logic.

Arrow terms are an extremely rich structure for representing quite different structures such as the way how the brain thinks, the way how to focus on customer needs by *Quality Function Deployment* (QFD), see Fehlmann (2002) and testing of complex, software-intense systems with thousands of *Embedded Control Units* (ECU).

## Acknowledgments

The authors would like to thank the anonymous referees for their valuable comments and suggestions which led to the improvement of the paper.

## References

Banach S, Tarski A (1924) Sur la décomposition des ensembles de points en parties respectivement congruentes. (On the decomposition of the sets of points into respectively congruent parts). *Fundamenta Mathematicae* 6(Jul): 244–277.

Barendregt HP (1977) The type-free lambda-calculus. In J Barwise (ed), 1091–1132. *Handbook of Math. Logic.* Amsterdam: North Holland.

Barwise J (1977) *Handbook of mathematical logic. Studies in logic and the foundations of mathematics.* Amsterdam, NL: North-Holland Publishing Company.

Bell D (2004) *UML basics: the sequence diagram – introductory level.* Armonk, NY: IBM DeveloperWorks.

COSMIC Measurement Practices Committee (2017) *The COSMIC functional size measurement method – version 4.0.2 – measurement manual.* Montréal: The COSMIC Consortium.

Curry H, Feys R (1958) *Combinatory logic.* Volume I. Amsterdam: North-Holland.

Curry H, Hindley J, Seldin J (1972) *Combinatory logic.* Volume II. Amsterdam: North-Holland.

Engeler E (1981) Algebras and combinators. *Algebra Universalis* 13(Dec): 389–392.

Engeler E (1995) *The combinatory programme.* Basel, Switzerland: Birkhäuser.

Engeler E (2019) Neural algebra on "how does the brain think?". *Theoretical Computer Science* 777(Jul): 296–307.

Fehlmann TM (1981) *Theorie und Anwendung des Graphmodells der Kombinatorischen Logik.* (Theory and application of the graph model of combinatorial logic). Zürich, CH: ETH.

Fehlmann TM (2002) QFD as algebra of combinators. *8th International QFD Symposium, ISQFD 2002, Tokyo, Japan.*

Fehlmann TM (2016) *Managing complexity - uncover the mysteries with six sigma transfer functions.* Berlin, Germany: Logos Press.

Fehlmann TM (2020) *Autonomous real-time testing - testing artificial intelligence and other complex systems.* Berlin, Germany: Logos Press.

Fehlmann TM, Kranich E (2019) Testing artificial intelligence by customers' needs. *Athens Journal of Sciences* 6(4): 265–286.

Fehlmann TM, Kranich E (2020) *A sensitivity analysis procedure for QFD.* Duisburg: (forthcoming).

Gunn S (1998) *Support vector machines for classification and regression.* ISIS Technical Report. Southampton: University of Southampton.

ISO/IEC 19761 (2011) *Software engineering - COSMIC: a functional size measurement method.* Geneva, Switzerland: ISO/IEC JTC 1/SC 7.

ISO 16355-1:2015 (2015) *Applications of statistical and related methods to new technology and product development process - part 1: general principles and perspectives of quality function deployment (QFD), Geneva, Switzerland: ISO TC 69/SC 8/WG 2 N 14.* Geneva, Switzerland: ISO TC 69/SC 8/WG 2 N 14.

Pawlikowski J (1991) The Hahn–Banach theorem implies the Banach–Tarski paradox. *Fundamenta Mathematicae* 138(1): 21–22.

Potter MD (2004) *Set theory and its philosophy.* Oxford, UK: Oxford University Press.

Rauglaudre Dd (2017) Formal proof of Banach-Tarski paradox. *Journal of Formalized Reasoning* 10(1): 37–49.

Robinson RM (1947) On the decomposition of spheres. *Fundamenta Mathematicae* 34(1): 246–260.

Saaty TL (2003) Decision-making with the AHP: why is the principal eigenvector necessary? *European Journal of Operational Research* 145(1): 85–91.

Tao T (2011) *An introduction to measure theory.* Los Angeles, CA: WordPress.com.

Zachos E (1978) *Kombinatorische Logik und S-Terme.* (Combinatorial logic and S terms). Zurich: ETH.

*Athens Journal of Sciences- Volume 7, Issue 3, September 2020 – Pages 159-174*

# Development and Implementation of a Sustainable IPM and Surveillance Program for the Invasive Tomato Leafminer, *Tuta Absoluta* (Meyrick) in Sudan

*By Mohammed E.E. Mahmoud[*], Ensaf S.I. Mohammed[±], Samira A. Mohamed[‡], Fathiya M. Khamis[+] & Sunday Ekesi[♦]*

*Tomato leafminer Tuta absoluta is a serious insect pest that originates in South America. In its transatlantic invasion it was first detected in Spain in 2006, then the pest rapidly invaded Africa threatening tomato production in the continent. Since its detection in Sudan in 2010, farmers relied heavily on insecticides to reduce the exploding population of the pest. An Integrated Pest Management Approach (Tuta IPM) to manage the pest was initiated by Agricultural Research Corporation (ARC) in collaboration with the International Center of Insect Physiology and Ecology (ICIPE) and financed by German Federal Ministry of Economic Corporation and Development (GIZ). The project aimed to determine distribution, host plants, natural enemies as well as to test some novel approaches to control T. absoluta. The study regarding spatial distribution showed that, the pest was found all over the country attacking mainly tomato, eggplant, potato, broad bean, watermelon, alfa alfa and other wild plants. Four parasitic hymenopteran parasitoids and two predatory bugs were reported as natural enemies attacking larval stage. Three types of pheromone proofed their efficacy in trapping males of T. absoluta were registered for commercial use. Deployment of male lures especially (Tuta optima®) in water traps in tomato fields from seedling to harvest reduced the population level of the pest as well as the fruit loss percentage to 5%. Water extract of Neem corticated seeds at (5% and 8%) and Khilla leaves reduced the number of insects/leaflet of tomato and the infestation percentage and augmented the yield. Intercropping of tomato with coriander and fenugrik reduced the infestation levels of tomato by T. absoluta and improved the quantity and quality of yield when compared to cultivation of tomato as sole crop. Obtained knowledge regarding the pest and its IPM package was disseminated to different stakeholders through filed guide books, brochures, Training of Trainers (TOT), field days and broadcasting programs.*

**Keywords:** *Tomato, leafminer, male lures, intercropping, botanical insecticides, knowledge dissemination*

[*]Associate Professor, Agricultural Research Corporation, Sudan.
[±]Agricultural Research Corporation, Sudan.
[‡]International Center of Insect Physiology and Ecology (ICPE), Kenya.
[+]International Center of Insect Physiology and Ecology (ICPE), Kenya.
[♦]International Center of Insect Physiology and Ecology (ICPE), Kenya.

## Introduction

Globally, Tomato (*Solanum lycopersicum*) is the most widely grown and consumed vegetables (Varela et al. 2003). The crop is grown for both the fresh fruit markets and the industrial processing. On other hand tomato is a valuable cash crop for income generation and is a major source of rural employment in the tropics. The crop is also a good source of vitamins and minerals for many impoverished malnutrition rural communities. In Sudan, tomato is second to onion in terms of production area and total annual production which estimated to reach 35,280 ha yielding 504,000 t per annum (Ahmed et al. 2001). Like in many African countries, tomato cultivation has a particular socio-economic significance as it offers employment opportunities for large sector of the rural communities involved in tomato production value chain. Several biotic and abiotic factors, however, constrained tomato production. Ranking high among the former are arthropod pests such as the red spider mite (*Tetranychus evansi*), African bollworm, (*Helicoverpa armigera*), leafminers (*Liriomyza spp*.) and thrips (*Frankliniella spp.*) (Dabrowski et al. 1994).

The problem of arthropods pest infestation in Sudan has been further compounded by the recent invasion by the South American micro lepidopteran moth (*T. absoluta*) in 2010 (Mohamed et al. 2012). As reported by (Mahmoud 2013) since its first detection in the country in a tomato greenhouse around Khartoum area, tomato leafminer has spread to many tomato growing regions of Sudan causing severe losses to the crop in glass houses and open fields ranged from 35% to 80% respectively. The primary management method for *T. absoluta* in various countries is largely based on the use of synthetic insecticides without any concern to the side effects that it may cause. The reliance on insecticides in different countries, has led to the development of resistance of *T. absoluta* to all classes of insecticides (Yalcin et al. 2015, Siquaria et al. 2000 and Lietti et al. 2005) and Africa is will likely to witness the same scenario if we continue use synthetic pesticides. Various natural enemies were reported associated with the pest worldwide and proofed their efficiency such as predatory bugs *Nesidiocoris tenuis* and *Macrolophus* found in the area of the Mediterranean and the Canary Islands, Tunisia, Algeria, Morocco, Egypt, Saudi Arabia, Iran, Israel and Korea (Linnavuori 1975, Luna and Wada 2011, Urbaneja et al. 2009, Zappala et al. 2012, Clavo et al. 2009).

Also different parasitoids especially braconids were recorded in many countries as a promising bio-agents to suppress the population of *T. absoluta* in various countries (EPPO 2005).

The use of botanicals; especially Neem *Azadirachta indica* which consists of Azadirachtin, a complex tetranortri-terpenoid, indicated their efficacy as anti-feedant, toxic and repellent to *T. absoluta* without any incidence of resistance was reported (Kona et al. 2014, Yalcin et al. 2015). Given the recent invasion history of the pest in Africa, ecological data such as distribution, population dynamic and host range is virtually lacking. Sound knowledge of such information represents the cornerstone for pest management. Also the pest being an alien to Africa there is less likelihood of occurrence of efficient natural enemies that can combat the

exploding population of this pest. Because *T. absoluta* has developed resistance to various classes of pesticides, the use of biorationals (including biopesticides and botanicals) is being recommended for management of the pest. For better understanding of all above prerequisites a program was formulated by Agricultural Research Corporation of Sudan in collaboration with International Center of Insect Physiology and Ecology and funded by GIZ with the following specific objectives:

- ✓ To establish the distribution, abundance, dynamics, host plants of *T. absoluta* in Sudan.
- ✓ To characterise the host range of *T. absoluta* in Sudan.
- ✓ To catalogue the indigenous natural enemies of *T. absoluta* across the country.
- ✓ To evaluate the trapping potentiality of some male pheromones.
- ✓ To evaluate performance of some insecticides against *T. absoluta* and its natural enemies.
- ✓ To test efficacy of different extracts of some botanicals for management of *T. absoluta.*
- ✓ To raise awareness about the pest and to recommend IPM package for its control.

The Phase 1 of the program started in 2012 and terminated in 2016. During the contract period various activities were concluded and the obtained findings of different objectives are as follows.

## Materials and Methods

### *Spatial Distribution of T. Absoluta*

Since its detection in Sudan 2010, surveys were conducted in different states in open fields and in glass house produced tomato in Sudan using male attractants in locally made water traps and using detergent as killer. The survey was conducted in tomato production areas in 13 states of Sudan. For each site longitude and latitudes were recorded using Magilan®GPS.

### *Host Plants of T. Absoluta*

In each area where traps were settled, each plant showed the symptoms of infestation by *T. absoluta* from the family Solanaceae or any other was collected, preserved in ventilated container and sent to the laboratory for investigation through rearing out. The emerged adults were identified using specific key.

*Temporal Distribution of T. Absoluta*

Tomato in Sudan is grown in summer and winter seasons, study regarding the seasonal abundance of *T. absoluta* was conducted in four states for early and late sown tomato.

In each study site, male pheromone water traps were deployed in the fields coincided with transplanting of tomato seedlings. Catches of traps were recorded weekly, traps water and detergent were renewed after recording the insects and the pheromones were renewed after 8 weeks as recommended by the manufacturer. Data regarding temperature were obtained from the adjacent Metrological Station.

*Natural Enemies of T. Absoluta*

Infested tomato plants by larvae of *T. absoluta* were collected and kept in ventilated containers and observed daily for the presence of parasitoids. Emerged parasitoids were collected, preserved in alcohol and sent to the Natural History Museum (NHM) UK for identification.

*Role of Sex Pheromones in Mass Trapping of T. Absoluta and Increasing Yield of Tomato*

Evaluation of the Effectiveness of Male Pheromones for Trapping *T. Absoluta*

Three Male lures TUA-Optima 0.8 mg; Tuta Long life and TUA-100N) were evaluated in two states in Sudan for their effectiveness on trapping males of *T. absoluta* using water traps; 24 pheromone traps/hectar, with detergent. The experiment was settled as Randomized Complete Block Design, the area for each treatment was 0.5 hectar and each treatment was replicated three times. All cultural practices were applied as recommended by Agricultural Research Corporation of Sudan and no any insecticide was applied during the whole study period. No of trapped males per trap per week was recorded and data were analysed using SAS statistical Computer based program and means were separated applying Duncan Multiple Range Test.

Role of Male Pheromones in Mass Trapping of *T. Absoluta*

Other study was conducted in 2 states (Dongola and Sennar) to determine the role of mass trapping of males of *T. absoluta* using pheromones in decreasing infestation and increasing yield of tomato in a participatory approach with farmers. Thousand pieces of pheromones were donated to farmers and installed in water traps with a detergent at dose rate 24 pheromone traps/hectar. The pheromone traps were deployed from the seedling stage of tomato up to the harvest and were renewed two times during the season. The yield

*Evaluation of the Efficacy of Some Insecticides to Control T. Absoluta*

Due to the reliance of farmers on insecticides for management of *T. absoluta*, trials were conducted in order to recommend and register effective insecticides

belonging to different groups. Consecutive trials were conducted to release some effective and safe use of insecticides in different Sudanese environment. Also, the role of some insecticides on the population of natural enemies was evaluated.

Insecticidal Potency of Water Extracts of Some Botanicals on *T. Absoluta*

The insecticidal activities of aqueous extracts of five local plants (Neem *Azadirachta indica*, Garlic *Allium sativum*, Argel *Solenostemma sp.*, Coriander *Coriandrum sativum* and Khella *Ammi visnaga* (L.) LAM plants) were evaluated against *T. absoluta* under greenhouse condition in comparison to standard insecticide (Biotrne 1.8% EC) and the untreated control in a Complete Randomized Block Design Experiment. The number of larvae of T. absoluta and infestation level of each treatment were recoded pre and post spray of different treatments.

Intercropping of Tomato with Coriander or Fenugreek for Controlling *T. Absoluta*

Also study was conducted to assess the effect of intercropping of tomato with coriander (*Coriandrum sativum* L.) or fenugreek *(Trigonellafoenum-graceum*) and compared to sole grown tomato in a Randomized Complete Block Design trial and same procedure applied above for evaluation was applied in this trial.

## Results and Discussion

*Distribution and Host Plants*

The survey for the distribution and host plants of *T. absoluta*, revealed the presence of the pest all around the country. *T. absoluta* was reported to be established and wide spread in Northern, River Nile, Khartoum, Sennar, Kassala, Gezira, White Nile, Blue Nile, North Kordofan, South Kordofan, Gedarif and Darfur States presented in Table 1 with high number of captured males ranged from 50 to 700 males/trap/day.

Surveys in Sudan confirmed that Tomato (*Solanum* lycopersicum) is the main host plant attacked severely by *T. absoluta* with loss percentages up to 100% (Figure 1A-B). Other cultivated host plants included eggplant, *S. melongena* L. (Figure 1C and Figure 2D); Potato, *S. tuberosum* L. (Figure 1D); alfalfa, *Medicago sativa* L.; Physic nut, *Jatropha curcas;* Broad bean, *Vicia faba* and Water melon, *Citrullus lanatus*. Also the pest was recorded attacking several wild plants that serve as represented alternative hosts. These include: Gubbain, *S. dubium* L.; Jimson weed, *Datura stramonium* L.; Common cocklebur (*ramtouk*), *Xanthium brasilicum* Vell and spiny amaranth, *Amaranthus spinosus* L. (Mohamed et al. 2015). *T. absoluta* infests all aerial parts of tomato plant with specific preference to leaves and fruits (Figure 2A-C).

**Table 1.** *T. Absoluta Sampling Sites across Sudan States using Tuta Optima (Male Attractant)*

| Area | State | Longitude | Latitude |
|---|---|---|---|
| **Faki Hashim** | Khartoum | 15 50 00.4 | 32 32 24.0 |
| **Elsaggay** | Khartoum | 15 56 22.5 | 32 33 49.9 |
| **Elgailly 1** | Khartoum | 16 00 56.6 | 32 34 14.3 |
| **Elgailly 2** | Khartoum | 16 01 21.3 | 32 35 10.9 |
| **Wad Ramli** | Khartoum | 16 06 28.9 | 32 34 30.3 |
| **Shambat** | Khartoum | 15 39 49.0 | 32 53 19.0 |
| **Abudelou Omdurman** | Khartoum | 16 03 30.7 | 32 0157.0 |
| **Kilo 7 Omdurman** | Khartoum | 15 44 13.3 | 32 20 56.0 |
| **Bagairailafoon** | Khartoum | 15 25 18.8 | 32 45 43.7 |
| **Wad Medani** | Gezira | 14 41 00.0 | 33 05 00.0 |
| **Um barouna** | Gezira | 14 25 49.3 | 33 33 28.2 |
| **Karaiba** | Gezira | 14 24 57.6 | 33 27 15.4 |
| **Shaygab** | Gezira | 14 25 56.6 | 33 27 26.4 |
| **DaimElmashaikha 1** | Gezira | 13 41 49.0 | 33 36 01.0 |
| **DaimElmashaikha 2** | Gezira | 13 41 44.8 | 33 36 15.0 |
| **Duffofa 1** | Northern | 19 33 01.4 | 30 27 17.6 |
| **Duffofa2** | Northern | 19 31 44.2 | 30 28 18.3 |
| **Artadi** | Northern | 19 09 40.4 | 30 28 18.2 |
| **Garada** | Northern | 19 16 18.5 | 30 36 59.2 |
| **Zaourat Middle** | Northern | 19 09 29.9 | 30 26 11.4 |
| **Zaourat north** | Northern | 19 20 02.4 | 30 25 0.30 |
| **Sennar** | Sennar | 13 56 00.0 | 33 06 00.0 |
| **Singa** | Sennar | 13 15 00.0 | 33 93 33.0 |
| **Kassala** | Kassala | 15 25 59.5 | 36 21 17.6 |
| **Takroof** | Kassala | 15 29 49.2 | 36 20 43.4 |
| **Kosti** | White Nile | 13 02 00.0 | 37 07 00.0 |
| **Shendi** | River Nile | 16 41 26.8 | 33 24 82.6 |
| **Shagalwa** | River Nile | 16 43 59.3 | 33 28 17.7 |
| **Ketiab** | River Nile | 16 43 53.8 | 33 28 25.8 |
| **Zeidab** | River Nile | 17 24 87.9 | 33 51 35.7 |
| **Singa** | Blue Nile | 13 09 08.4 | 33 56 44.7 |
| **Azazah 2** | Blue Nile | 13 06 56.3 | 33 57 53.9 |
| **Elhawata** | Gedarif | 13 25 10.6 | 34 37 56.1 |
| **Bazoura** | Gedarif | 13 06 32.8 | 34 55 91.2 |
| **Gadoura 2** | Gedarif | 13 00 12.2 | 34 58 00.3 |
| **Elgazira aba** | White Nile | 13 20 36.6 | 32 36 38.5 |
| **Almakhaleef** | White Nile | 12 29 37.9 | 32 49 13.3 |
| **Eldiuem** | White Nile | 12 49 58.0 | 32 47 25.0 |
| **Nyala** | S. Darfur | 12 01 55.4 | 24 55 48.9 |
| **Elgenaina** | W. Darfur | 13 26 46.6 | 22 27 49.1 |
| **Zalenji** | C. Darfur | 12 04 21.6 | 23 08 08.7 |

**Figure 1.** *Infestation Symptoms of T. Absoluta on: A-top left) Tomato in Open Field, B-top right) Tomato in Glass House, C-bottom left) Eggplant Field, D-bottom right) Potato Field*

**Figure 2.** *Infestation Symptoms of T. Absoluta* on: *A-top left) Leaves of Tomato, B-top right) Flower and Buds of Tomato, C-bottom left) Fruit of Tomato, D-bottom right) Fruit of Eggplant*

*Seasonal Abundance of T. Absoluta on Tomato*

For both sowing times, the population of insect increased gradually during vegetative growth of the plant coincided with the increase of temperature up to 30 $C^{o}$ and flared up during the fruiting time and increased steadily to reach the crest during the second and third picking of fruits (Figures 3-5). The pest was found all around the year which is coincided with the information provided by Elhaj et al. (2015) who reported that *T. absoluta* can be found all the year round in greenhouses and in locations with mild winters.

**Figure 3.** *Average Number of T. Absoluta of the Early Sown Tomato from December to February (2012/2013) for Three Locations in Kassala State*

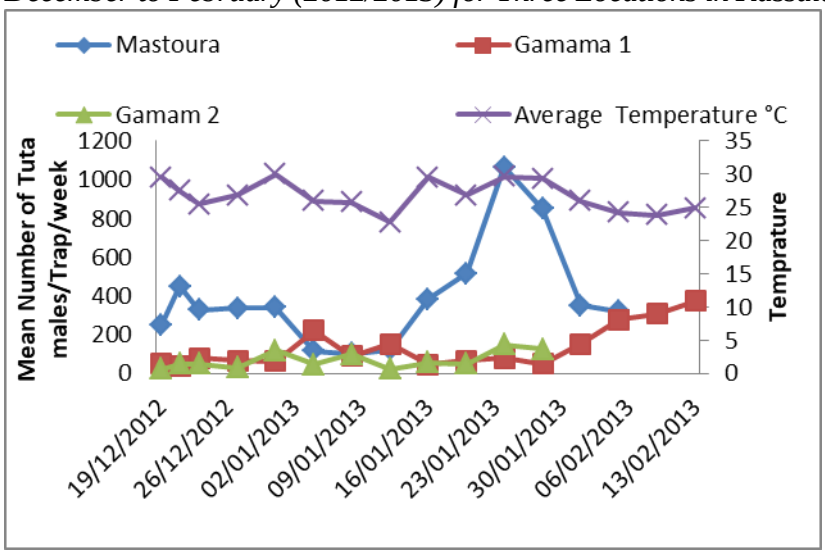


**Figure 4.** *Average Number of T. absoluta Trapped Males for the Late Sown Tomato from February to June 2013, Khartoum State Natural Enemies of T. Absoluta in Sudan*

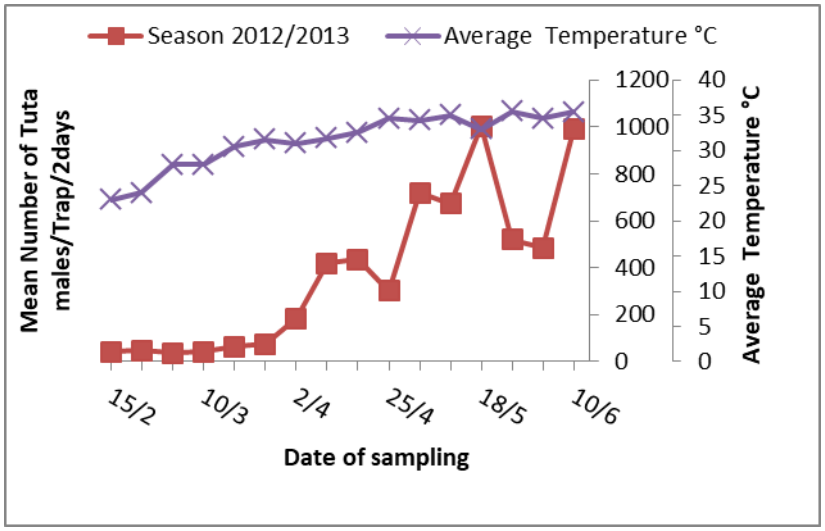

**Figure 5.** *Average Number of T Absoluta Trapped Males of Three Season for the Early Sown Tomato from December to March, Season 2013/2014 (Senna State)*

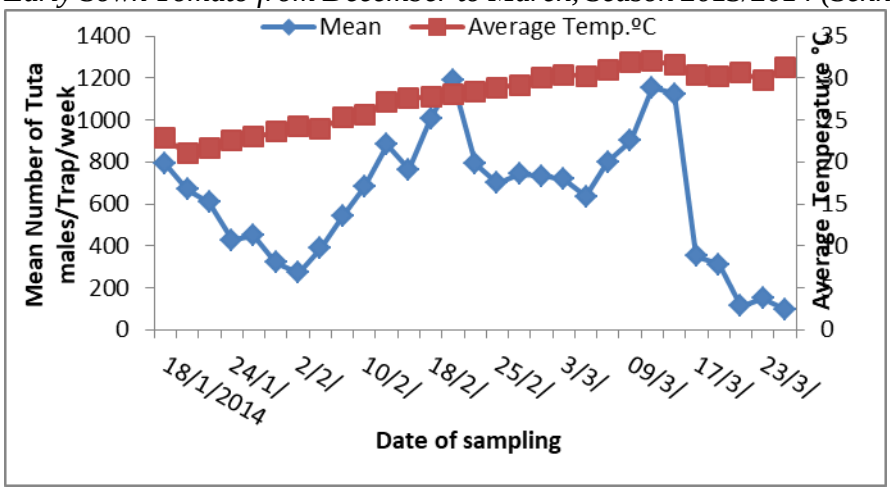


The survey for natural enemies across different states in Sudan revealed the form of new association between five hymenopteran parasitoids with *T. absoluta*. These parasitoids are *Bracon* (Habrobracon) sp. *Concolorans* Marshall (Figure 6A), *Bracon (Habrobracon) hebetor* Say (Figure 6B); Torymidae *Ecdamuacadenati* (Risbec) all the three species belonging to the family Braconidae. Also *Neochryso-charisformosa* (Westwood) of the family Eulophidae was reported as parasitoid of *T. absoluta.* Also, *Macrolophu ssp.* (Figure 6C) and *Nesidiocoris tenuis* (Figure 6D) are found as very efficient predatory bugs preying on eggs and larvae of the pest.

**Figure 6.** *Natural Enemies of T. Absoluta A-top left) Bracon (Habrobracon) hebetor, B-top right) Bracon Nigricans, C-bottom left) Macrolophu ssp., D-bottom right) Nesidiocoris Tenuis*

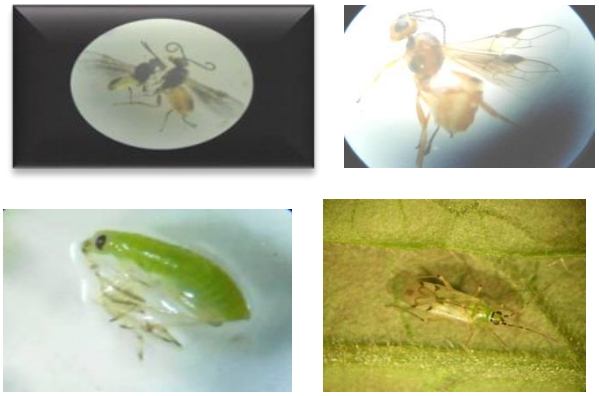

**Trapping of *T. Absoluta***

*Evaluation of the Effectiveness of Male Pheromones for Trapping of T. Absoluta*

The results of evaluation of the performance of the three lures for trapping males of *T. absoluta* showed that, the three lures are potent attractants to the males of *T. absoluta*. TUA-Optima® loaded with 0.8 mg had the higher captures of males at both study sites followed by Tuta Long life® and TUA-100N®, (Figure 7). TUA-100N® and Tuta long life are new slow release pheromone system that can last up to 100 days. These two products are designed for open field tomato cultivations in the hot climates. The use of the three pheromones reduced the level of infestation to 18%, 22%, 28% for Tuta optima®, Tua 100N®, Tuta long life® respectively, while the infestation level for the control plots was 55%. The results of males mass trapping resulted in yield increase and enrichment of tomato fruits quality.

*Role of Male Pheromones in Mass Trapping of T. absoluta*

The experiment of mass trapping of males of *T. absoluta* which was conducted in two states using pheromone traps resulted in capturing of high numbers of males during vegetative growth which reflected positively in reducing the number of catches during the fruiting season and lowered the infestation levels of tomato fruits in the two states to 5±0.5 % and to 3.5±03% in Sennar State sites. The obtained results in this trial is in accordance with the findings of Benvenga et al. (2007) and Mohamed and Mahmoud (2013) who stated the possibilities of using pheromone traps in mitigating the population of *T. absoluta*.

It was obliviously recorded that, the use of pheromone in trapping males of *T. absoluta* increased the population of natural enemies especially the predatory bugs *Macrolophus* and *Nesibug* (Figure 8).

**Figure 7.** *Catchability of Pheromones to Males of T. Absoluta in Tomato Field, Sudan*

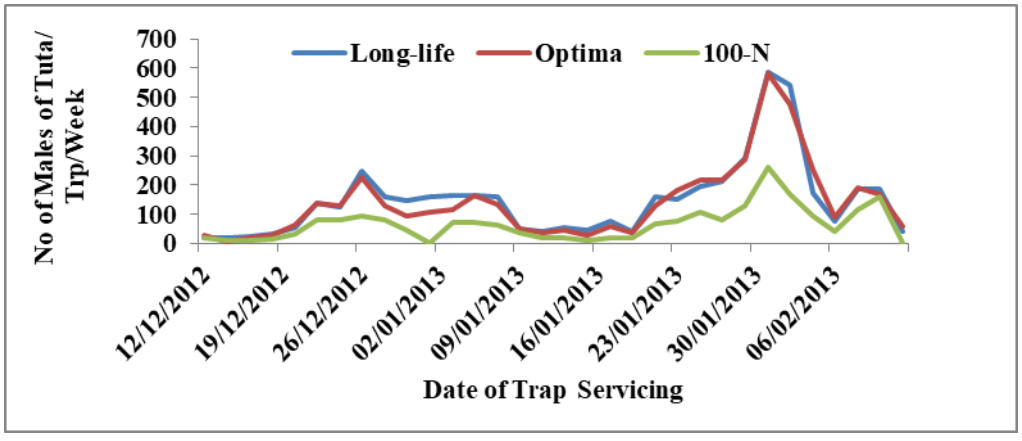

**Figure 8.** *Effect of Using Pheromones for Trapping Males of T. Absoluta on the Population of Natural Enemies*

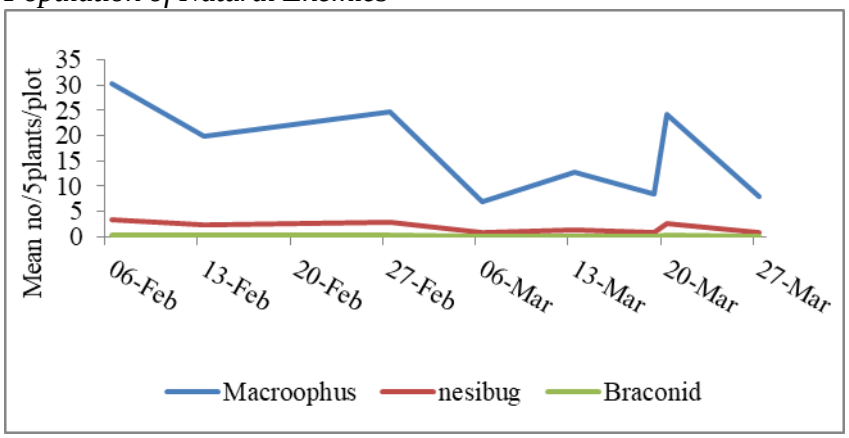


*Evaluation of the Efficacy of Some Insecticides to Control T. Absoluta*

After consecutive trials some insecticides were registered and released to be applied by farmers to control tomato leafminer among them are Spinosad, Belt Extra (Spirotetramat + flubendiamide), Indoxicarb, Acetamiprid products, Abamectin and Emamectin benzoate products. Study regarding the effect of insecticides on the population of *T. absoluta* and natural enemies reflected that, most of insecticides reduced the population of the pest and at same time affect negatively the population of natural enemies of *T. absoluta* (Figure 9).

**Figure 9.** *Effect of Insecticides used to Control T. Absoluta on the Population of Natural Enemies*

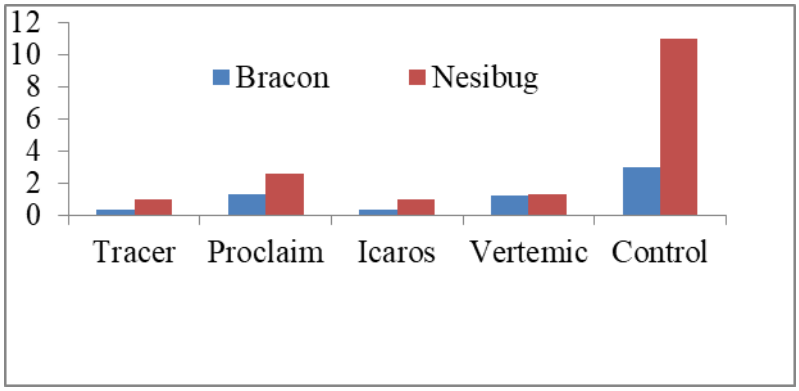


*Insecticidal Potency of Water Extracts of Some Botanicals on Tomato Leafminer Management*

Regarding the use of water extracts of botanicals to control Tomato leafminer, all tested aqueous extracts of the test plants reduced the number of infested leaflets of tomato plants, the number of mines on tomato plants and the number of infested fruits/plants compared to the untreated control. Aqueous extract of Neem 5% was significantly better than Biotrne 1.8% EC and other botanicals in all above

mentioned insect parameters. On other hand the use of Neem reflected positively in reduction of yield loss in tomato fruits due to the infestation of *T. absoluta* to less than 10% followed by Biotrne 1.8% EC (Figure 10).

**Figure 10.** *Effect of Using Water Extract of Some Botanicals to Control T. Absoluta in no of Infested Leaflets/Plant, no of Mines/Plant, no of Infested Fruits/ Plant and Percentages of Yield Loss*

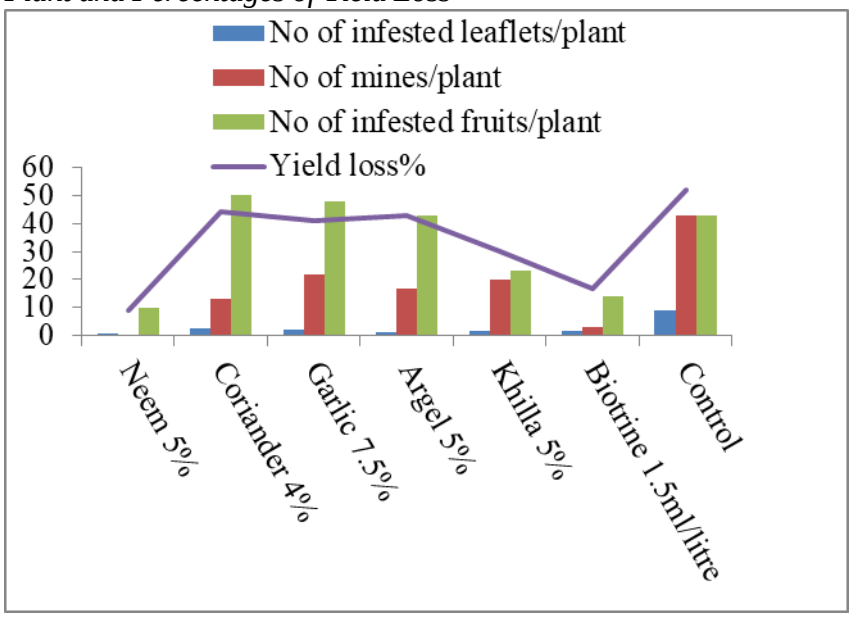


*Intercropping of Tomato with Coriander or Fenugreek for Controlling T. Absoluta*

The intercropping experiment indicated that, the use of coriander or fenugreek intercropped with tomato lowered the number of infested fruits when compared to mono-cropped tomato.

**Capacity Building and Public Awareness**

Within the program of IPM of *T. absoluta*, six training of trainers (TOTs) were conducted in 6 states of Sudan for 240 trainers. The trained persons were staff of Plant Protection Directorate, Universities teaching staff, extension officers, Agricultural Research staff and pioneer farmers (Figure 11). The gender issue was considered where 40% of the participants were females. Ten field days attended by more than 1,200 farmers were conducted. In the field days, the farmers were acquainted with knowledge on the pest biology, host range, natural enemies and eco-friendly control tactics to reduce the damage caused by *T. absoluta*.

Also, public awareness was raised through several radio and T.V programs at national and state levels giving information about the pest, prospects of its integrated management and safe use of insecticides.

**Figure 11.** *Activities of Capacity Building Include TOT, Farmers Field Schools and Field Days*


## Conclusions

Tomato leafminer is well established in Sudan and become the main constrain that reduce tomato productivity all over the country. Successfully, strenuous efforts resulted in adding *T. absoluta* to the list of the national pests which are managed by the federal government authorities to reduce the reliance of farmers on insecticides and help the poorest farmers by offering pheromone traps in free of charge basis.

The results obtained in the first phase of this project highlighted the promising role which natural enemies can play especially the predatory bugs (Nesibug and mirid bug) and braconid parasitoids. Further studies regarding their efficacy and suitability as indigenous parasitoids should be well studied in order to be mass reared and released to suppress the population of *T. absoluta*.

From the results obtained also Use of pheromone/s in mass trapping of *T. absoluta* was found a key control measure that should be considered as a corner stone in any IPM program for the quick action it cause in the tremendous reduction of the population of *T. absoluta*, indirect increase of the population of natural enemies and maximization of the produce and alleviating it to the standards of organic product. Time of application is considered as the most important factor for the successful of mass trapping operations. It is preferred to start monitoring the population of *T. absoluta* from the sowing date or transplanting of seedlings and start mass trapping after the population reach 30 males/trap/week.

The registration of some insecticides from different chemical groups will help particularly in providing alternatives to reduce the chances of generation of

resistance of *T. absoluta* to the action of insecticides as the pest known to show resistance to most of insecticides especially that belonging to organophosphate and pyrethroid groups.

According to the obtained results of the efficacy of water extract of Neem on controlling *T. absoluta.* Using different extracts of neem tree for the purpose of controlling this pest should be given more attention by the scientists for the abundance of neem tree all around the year.

Intercropping of tomato with coriander and/or fenugreek which gave good performance in controlling *T. absoluta* is one of the techniques that can be adopted by farmers as push and pull strategy, in Sudan spices such as coriander and fenugreek are of high economic value, where they can regenerate money for farmers and compensate the loss of tomato yield.

Due to the ravage damage it causes and quick movement and invasive behavior, integration of all control options is the key role to the management of *T. absoluta.* Screening of different tomato genotypes for resistance to tomato leafminer, identification and introduction of endophyte/s and entomopathogens and assess the role of natural enemies and develop procedure for mass rearing of the most promising one/s to be applied in bio-control program will play the utmost role to management of the best, secure and safe food.

## Acknowledgments

Authors would like to thanks German Federal Ministry of Economic Corporation and Development (GIZ) for their generous fund and also extended their thanks to farmers all around the country for their keen help and provision of information.

## References

Ahmed NE, Kanan HO, Sugimoto Y, Ma YQ, Inanaga S (2001) Effect of imidacloprid on incidence of tomato yellow leaf curl virus. *Plant Disease* 85(1): 84–87.

Benvenga SR, Fernandes OA, Gravena S (2007) Decision making for integrated pest management of the South American tomato pinworm based on sexual pheromone traps. *HorticulturaBrasiliera* 25(2): 164–169.

Calvo J, Bolckmans K, Stansly PA, Urbaneja A (2009) Predation by *Nesidiocoris tenuis* on Bemisiatabaci and injury to tomato. *BioControl* 54(2): 237–246.

Dabrowski ZT, Alsaffar A, Abderahman AA (1994) Integrated pest management on vegetable crops in sudan: development and implementation strategy. In: ZT Dabrowski (Ed), Pages 24–32. *Integrated Vegetable Crop Management FAO/ Government of the Sudan Cooperative Project, GCD/ SUD/02A/NET*. Nairobi, Kenya: ICIPE Science Press.

Elhaj M, Abdelbagi AO, Ahmed MA, Mahmoud MEE (2015) Seasonal abundance and host range of tomato leaf miner *Tuta absoluta* Meyrick (lepidoptera: gelechiidae). *The Journal of Agriculture and Natural Resources Sciences* 2(Jan): 2423–4397.

EPPO (2005) Tuta absoluta. *EPPPO Bulletin* 35(3): 434–435.

Kona NEM, Taha AK, Mahmoud MEE (2014) Effects of botanical extracts of neem (*Azadirachtaindica*) and jatropha (Jatropha curcus) on eggs and larvae of tomato leaf miner, Tuta absoluta (Meyrick) (lepidoptera: gelechiidae). *Persian Gulf Crop Protection* 3(3): 41–46.

Lietti M, Botto E, Alzogaray R (2005) Insecticide resistance in Argentine populations of Tuta absoluta (Meyrick) (lepidoptera: gelechiidae). *Neotropical Entomology* 34(1).

Linnavuori RE (1975) Hemiptera of the Sudan, with remarks on some species of the adjacent countries: 4. Miridae and isometopidae. *Annales Zoologici Fennici* 12(1): 1–118.

Luna MG, Wada VI (2011) Neochrysocharisformosa (Westwood) (Hymenoptera: Eulophidae), a newly recorded parasitoid of the tomato moth, Tuta absoluta (Meyrick) (lepidoptera: gelechiidae) in Argentina. *Neotropical Entomology* 40(3): 412–414.

Mahmoud MEE (2013) Natural enemies of *Tuta absoluta* in Kassala. Presented in *Tuta Absoluta: Meeting the Challenge of the Tomato Leafminer, Intercontinental Hotel, Addis Ababa, Ethiopia, Tuesday, November 26, 2013*.

Mohamed ESI, Mahmoud MEE (2013) Evaluation of pheromone lures for mass trapping of the tomato leafminer, Tuta absoluta in tomato under open field and greenhouses in Sudan. Presented in *Tuta Absoluta: meeting the Challenge of the Tomato Leafminer, Intercontinental Hotel, Addis Ababa, Ethiopia, Tuesday, November 26, 2013*.

Mohamed ESI, Mohamed ME, Gamiel SA (2012) First record of the tomato leafminer, *Tuta absoluta* (Meyrick) (lepidoptera: gelechiidae) in Sudan. *EPPO Bulletin* 42(2): 325–327.

Mohamed ESI, Mahmoud MEE, Elhaj MAM, Mohamed SA, Ekesi S (2015) Host plants record for tomato leaf miner Tuta absoluta (Meyrick) in Sudan. *Bulletin OEPP/ EPPO* 45(1): 108–111.

Siqueira HAA, Guedes RNC, Picanço MC (2000) Insecticide resistance in populations of Tuta absoluta (lepidoptera: gelechiidae). *Agricultural and Forest Entomology* 2(2): 147–153.

Urbaneja A, Monton H, Molla O (2009) Suitability of the tomato borer Tuta absoluta as prey for Macrolophuspygmaeus and *Nesidiocoris tenuis*. *Journal of Applied Entomology* 133(4): 292–296.

Varela P, Gámbaro A, Giménez AM, Durán I, Lema P (2003) Sensory and instrumental texture measures on ketchup made with different thickeners. *Journal of Texture Studies* 34(3): 317–330.

Yalçin M, Mermer S, Kozaci L, Turgut C (2015) Insecticide resistance in two populations of *Tuta absoluta* (Meyrick, 1917) (lepidoptera: gelechiidae) from Turkey. *Turkish Journal of Entomology* 39(2): 137–145.

Zappala L, Bernardo U, Biondi A, Cocco A, Deliperi S, Delrio G et al. (2012) Recruitment of native parasitoids by the exotic pest *Tuta absoluta* in Southern Italy. *Bulletin of Insectology* 65(1): 51–61.

*Athens Journal of Sciences- Volume 7, Issue 3, September 2020 – Pages 175-194*

# Dark Energy and Matter as Essential Components of the Expanding Universe

*By Dipo Mahto[*], Bijay Kumar[±], Umakant Prasad[‡], Brajnandan Kumar[+], Supriya Kumari[♦] & Sanjay Kumar Choudhary[°]*

*The present work reviews the facts of some models related to the dark matter and energy with variation of gravitational and cosmological constants with the cosmic time by giving the evidence in support of expanding universe due to Big Bang. Three important time epochs of BBN like Inflationary era, Radiation dominated era and Matter dominated era have also been discussed. The paper discusses also about the age of the universe using Hubble law in terms of Hubble constant and density parameter including the concept of space-time, geography of the universe, new cosmology, dark energy and some challenges and says that the correct theory of gravity is massive scalar-tensor gravity drawn from the detection of the gravitational wave from the collision of binary black holes as predicted by Albert Einstein's general theory of relativity, 100 years ago.*

**Keywords:** *Dark energy, dark matter, gravitational & cosmological Constant*

## Introduction

Edwin Hubble demonstrated that the spiral nebulae observed in the telescope are in the fact galaxies like the Milky Way (Hubble 1926). He showed that the spectral lines of most galaxies are shifted towards the red, which suggests that they are moving away to each other in all possible directions and the universe is expanding (Hubble 1929, 1982). On the basis of the Hubble diagram, it is clear that the red shift of the galaxy is directly proportional to the distance indicating that the higher the red shift more distant the galaxy (Kirshner 2004). The recent observations show that there are about$10^{22}$ to $10^{24}$ galaxies and they have wide range in size. Each galaxy contains approximate $10^{11}$-$10^{12}$ stars (Staff 2019). The theoretical calculations based on the general theory of relativity led the big-bang theory which suggested that the universe has expanded from a very hot, very dense state existing at some finite time about 14 billion years ago in the past (A142 2012). Zwicky (1933) showed that the visible matter accounts for only a tiny fraction of all of the mass in the universe during 20$^{th}$ century (Zwicky 1993). Kahn and Woltjer (1959) pointed out that M 31 and the Galaxy were moving towards each other so that they must have completed most of an orbit around each other

[*]Associate Professor, Department of Physics, Marwari College, T.M.B. University, India.
[±]Graduate Teacher, Simultala Awasiya Vidyalaya, India.
[‡]Associate Professor, Department of Physics, T.N.B. College, T.M.B. University, India.
[+]Research Scholar, Department of Statistics, T.M.B. University, India.
[♦]Assistant Professor, Department of Physics, SBN College, India.
[°]Principal, T.N.B. College, T.M.B. University, India.

during a Hubble time (Kahn and Woltjer 1959). Wang (1991) studied the astrophysical bounds on the change of the gravitational constant with time and found that $\dot{G}/G = 10^{-12}\,yr^{-1}$ is the condition that has to be satisfied in order not to cause a conflict with the observations (Wang 1991). Singh and Agrawal (1993) studied the Einstein field equations with perfect fluid source and variation of cosmological and gravitational constants with cosmic time for Bianchi-type universe (Singh and Agrawal 1993). Melek (2000) studied the limits on cosmic time-scale variations of gravitational and cosmological constants regarding the spatially perturbed FRW metric (Melek 2000). Boyle et al. (2002) investigated a class of models for dark matter and negative pressure, dynamical dark energy consisting of "spintessence" a complex scalar field spinning in a U(1) symmetrical potential (Boyle et al. 2002). Singh (2006) considered the Einstein field equitation in zero-curvature R-W Cosmology with perfect fluid source and time-dependent gravitational and cosmological constants (Singh 2006). Buchert (2008) described the effective evolution of an inhomogeneous universe models in any theory of gravitation in terms of spatially averaged variables (Buchert 2008). Aguirre (2008) reviewed the initial condition for the standard cosmology model and gave confrontation of this theory with observations of the Cosmic Microwave Background (CMB) (Aguirre 2008). Bilic (2010) discussed the thermodynamic properties of dark energy in terms of a self-interacting complex scalar (Bilic 2010). Silva et al. (2011) discussed thermodynamic properties of dark energy components assuming a general time-dependent equation of state parameters (Silva et al. 2011). Dallal and Azzam (2012) discussed that the discovery of the Higgs boson had provided new momentum for the Standard Model as a cornerstone in understanding the universe (Dallal and Azzam 2012). Bilic (2011) studied a non-interacting supersymmetric model in de Sitter space-time providing matching between the vacuum energy density and the cosmological constant to the de Sitter expansion parameter (Bilic 2011). Shaikh and Wankhade (2015) discussed a dark energy model with EoS parameter for hypersurface-homogeneous space-time filled with perfect fluid source in the frame work of f(R,T) gravity (Shaikh and Wankhade 2015).

In the present work, we have reviewed the fact regarding some models related to the dark matter and energy with the variation of Gravitational and cosmological constants with cosmic time giving the evidences in support of expanding universe due to Big Bang. Three important time epochs of BBN like Inflationary era, Radiation dominated era and Matter dominated era have been discussed. We also have discussed about the age of the universe using Hubble law in terms of Hubble constant and density parameter with the concept of space-time, geography of the universe, New Cosmology, Dark energy and some challenging issues that we had to face in predicting the secret of expanding universe.

## Concepts of Space and Time

The Newtonian mechanics defines the space and time as rigid and immutable. This means that the space and time is absolute. The concept of space and time in general theory of relativity differs from the Newtonian space time. According to general theory of relativity, the structure of the space time is affected by the presence of matter and hence it becomes soft and malleable. In the String theory, the coupling constants are determined by the vacuum expectation values of some scalar fields and hence they are no longer constant at all. Regarding this theory, the space and time can be viewed as a frame work for softening the laws of physics. This can be summarized as follows (Chiba 2011).

**Table 1.** *Concept of Space & Time*

| S. No. | Theory as proposed | Space | Time |
|---|---|---|---|
| 1. | Newtonian Theory | Rigid | Rigid |
| 2. | Einstein Theory | Soft | Rigid |
| 3. | String Theory | Soft | Soft |

We know that the universe is expanding just like balloon expands in all possible directions. Hence the parameters like the gravitational constant, cosmological constant. Hubble constant and energy density are varying with cosmic time from the evolution of the Universe. Any detection/non-detection for the variations of all above parameters could provide useful information about the nature of dilation/moduli fixing and the coupling of the quintessence field. The quintessence is meant by the cosmic acceleration induced by a slowly rolling light scalar field and this can couple the electromagnetic field and gravitational field. Due to this reason, we discuss about the parameters discussed above.

## Geography of the Universe

The entire universe consists of $10^{11}$ galaxies. Each galaxy has $10^{11}$ stars, few black holes, neutron stars, white dwarfs and other asteroids. The entire universe is just like balloon and expanding so that stars of the galaxy are receding to each other. In comparison to the stars in any galaxies, the black holes, neutron stars, white dwarfs, etc., are few in numbers. The star is the basic building blocks of the universe. A galaxy has luminous centre containing nearly all stars and a dark halo of unknown compositions. In the most of cases, there is a nucleus consisting of black holes which is gobbling up stars and gas and emitting radiation. When the nucleus is the dominant feature, then it is known as an AGN. Seyfert galaxies and quasars belong to this category. Generally, large galaxies have a size of .1 Mpc and are of order 1Mpc apart. Many galaxies belong to gravitationally bound clusters containing from 2 to1000 galaxies. Small clusters are usually called groups. Big clusters are the biggest gravitationally bound objects in the universe. The biggest distance can be observed in the order of $10^4$ Mpc. The observable

universe is extremely homogenous and isotropic and closed analogous to the surface of an extremely deformed sphere. The universe is expanding isotropically. In the astronomy, the astronomers use the unit Mega parsec to measure the astronomical distance as follows (David 1993):

$1pc = 3.26\ \ light\ \ years = 3.09 \times 10^{16} meters.\ \ 1Mpc = 10^6\ pc$,

The mass of stars are ranging roughly from $1M_\oplus$ to $10M_\oplus$. This range may be $10^6 M_\oplus$ to $10^{12} M_\oplus$ for dwarf and large galaxies respectively.

**Big Bang Nucleosynthesis**

Big Bang nucleosynthesis (BBN) is known as primordial nucleosynthesis. This is one of the most important pillars of the modern cosmology and testing ground upon which many cosmological models must ultimately rest (Patrignani et al. 2016). Primordial nucleosynthesis process has taken place after the Big Bang in the interval from roughly 10 seconds to 20 minutes and the most part of the helium of Universe are formed as the isotope helium ($^4He_2$) along with small amounts of the hydrogen isotope deuterium ($^2H_1$ or D), the helium isotope helium ($^3He_2$), and a very small amount of the lithium isotope lithium-($^7Li_3$). In this process, two unstable or radioactive isotopes named the heavy hydrogen isotope tritium ($^3H_1$ or T); and beryllium isotope beryllium-7 ($^7$Be) were also produced. These two unstable isotopes later decayed into $^3He_2$ and $^7Li_1$ (Coc and Vangioni 2017).

There are three important time epochs of BBN as follows (Mathews et al. 2017):

1. Inflationary era: In this stage, the energy density is dominated by the potential of a scalar field. In this era. In this stage, the time is about $10^{-2}$ second and temperature is approximately equal to 10MeV and the energy density of the universe is dominated by relativistic particles like neutrinos, antineutrinos, positive electrons and negative electrons in thermal equilibrium. In this era, the weak interaction rates are faster than the universal expansion rate.
2. Radiation dominated era: In this stage, the energy density is dominated by relativistic particles called radiation. In this stage, the time is about 1 second and temperature is approximately equal to 1MeV and the radiation density of the universe is dominated by relativistic particles like proton, neutron, neutrinos, antineutrinos, positive electrons and negative electrons in thermal equilibrium. In this era, the weak interaction rates can no longer maintain the thermal equilibrium. The reactions are as follows:

$$n + \nu_e \Leftrightarrow p + e^-$$
$$n + e^+ \Leftrightarrow p + \nu_e^-$$
$$n \Leftrightarrow p + \nu_e^- + e^-$$

3. Matter dominated era: In this stage, the energy density is dominated by the mass of non-relativistic particles called matter. At the temperature from T=0.5 to 0.1MeV, positive and negative electron pairs begin to annihilate the photon gas. The neutrino gas is however, unaffected by this time. At t=100s, the n/p ratio has diminished from 1/6 to 1/7 by neutron decay, then the helium mass fraction becomes approximately equal to 0.25 which is very close to observed abundance.

The best current understanding of the composition of the universe comes from the analysis of the Planck Surveyor. When combined analysis of the Planck temperature plus polarisation and gravitational lensing data with Baryan Acoustic Oscillation in the matter power spectrum and supernovae data from the Joint Light-Curve analysis of type Ia supernovae is taken into consideration, then, we obtain

$$\Omega_b h^2 = 0.02230 \pm 0.00014$$

where $h = 0.6774 \pm 0.0066$. The other key quantity to study for the formation of the universe starting from BBN is a term called $\eta$ representing the ratio of the baryon number density to the photon number density, which relates the quantity $\Omega_b h^2$. The calculated value of $\eta$ concludes that there are about 400 photons per $cm^3$ in the universe and roughly 2 billions photons per baryon. This number was fixed in the epoch of baryon-genesis. From the Planck analysis, the baryonic is $\Omega_b = 0.0486 \pm 0.011$, total matter content is $\Omega_m = 0.3089 \pm 0.062$ and completely unknown component of cold dark matter is $\Omega_c = 0.260 \pm 0.006$ are calculated. In addition to above analysis, the universe is predominantly made completely exotic form of mass energy called dark energy denoted by $\Omega_\Lambda = 0.691 \pm 0.006$. There are some other contribution of presence of matter due to relativistic photons and neutrinos given by $\Omega_\gamma = 5.46 \times 10^{-5}$ (Planck Collaboration 2016). Thus, we see that the composition of present universe is a great cosmic mystery and about 95% form of matter of the universe called Dark matter & Energy are present about which we have little Knowledge. Now a day, this subject is a challenge for the Astrophysicists and cosmologists to solve this puzzling matter.

## The Age of the Universe

The universe is expanding isotropically so that the distance between any pair of the galaxies separated by more than 100Mpc is proportional to a universal scale factor a(t). The Hubble parameter is defined as

$$H = \dot{\alpha} / \alpha, \qquad (1)$$

where dot is the time derivatives. The present value of H is $H_0$ known as Hubble constant. The galaxies are receding from us with velocity $v << 1$ can be measured by the red shift $z \equiv \Delta\lambda / \lambda$ and velocity of such galaxies is given by

$$v = Hr. \qquad (2)$$

The Hubble constant $H_0$ is in the range from 40 to 100km/sMpc$^{-1}$ and defining a quantity h so that as $H_0$==100hkm/sMpc$^{-1}$. The red shift determination gives 0.4< h <1. Since, $H = \dot{\alpha} / \alpha$, the time taken for the universe to expand by an appreciable amount is of order the Hubble time given by following

$$H_0^{-1} = 9.7h^{-1} \times 10^9 \, Mpc \qquad (3)$$

During the Hubble time, the light travels a distance of order the distance given by the following equation

$$H_0^{-1} = 2998h^{-1} Mpc \qquad (4)$$

Hubble law holds good only for those galaxies whose distance is much less than the Hubble distance. This principle is based on the non-relativistic Doppler shift and it requires $v << 1$. At the present the epoch, the Hubble time is of order $10^{10}$ years. When we go back to an era, when the universe was very hot and dense, the estimation and theoretical calculation shows that the Hubble time was only a tiny fraction of second and popularly known as the Hot Big Bang. It is presumably assumed that when the Hubble time is of order the Planck time given by the following equation

$$t_{Pl} = G^{1/2} = 5.39 \times 10^{-44} \sec. \qquad (5)$$

then it is known as the Planck epoch.

From the study of the nucleo-synthesis, baryonic matter contributes the density parameter $\Omega_o = 0.01 - 0.09$. The theoretically favoured value of density parameter is $\Omega_o = 1$. This fact indicates the presence of non-baryonic dark matter in addition to baryonic dark matter. The luminous matter accounts for only $\Omega_o = 0.01$. Even if $\Omega$ is not equal to1 at the present epoch, it quickly approaches 1 as we go back in time. If the density parameter $\Omega_o << 1$, then we are able to estimate the epoch before which $\Omega$ is practically equal to 1 as follows:

As long as $\Omega_o << 1$, the gravity is negligible and therefore $\dot{\alpha}$ is constant, leading that

$$H \propto \alpha \qquad (6)$$

and

$$\Omega \propto \rho / H^2 \propto \alpha^{-1} \quad (7)$$

If $\Omega$ is approximately equal to 1 before the epoch, then

$$\alpha \equiv \Omega_0 \quad (8)$$

Since $\Omega_o \geq 1$, we see that $\Omega$ is certainly close to 1 before $\alpha \equiv 0.1$.

The Friedmann equation allows to calculate the present age of the universe in terms of $\Omega_o$ and for $\alpha = \Omega_o$, we have

$$\alpha \propto t^{2/3} \text{ at H=2/3t} \quad (9)$$

Therefore

$$t_0 = \frac{2}{3} H_0^{-1} = 6.5 \times 10^9 h^{-1} year \quad (10)$$

If $\Omega_o = .1$, then we have

$$t_0 = .9 H_0^{-1} = 8.8 \times 10^9 h^{-1} year \quad (11)$$

where

$$h<0.65 \text{ for } \Omega_o = 1 \text{ and } h<0.88 \text{ for } \Omega_o = .1 \quad (12)$$

Using the Hubble law, different astronomers estimated the value of h as .4<h<1, but the true value of h is as:

$$0.40<h<0.65 \quad (13)$$

## Theoretical Discussion

The evolution of the universe is described by Einstein field equations together with perfect fluid and equation of state in the relativistic and observational cosmology. Einstein's theory of gravitation involves two fundamental constants called Newtonian gravitational constant and cosmological constant (Singh 2006). These two fundamental constants have vital role to explain about the evolution of the universe. The variation of these two constants with cosmic time gives us the

idea about the expanding universe initially from Big-Bang. The Gravitational constant (G) and Cosmological constant $(\Lambda)$ may be defined as: When two bodies of unit mass are placed at unit distance, the force of attraction acting between them is called the gravitational constant (Mahto et al. 2013), while the homogeneous energy density of the vacuum that causes the acceleration of expansion of the universe is called the Cosmological constant (Davis and Griffen 2010). This cosmological constant $(\Lambda)$ was assumed to zero by the most cosmology researchers from 1929 to 1990 $(\Lambda = 0)$, but the supernovae explosion in 1998 has shown that about 68% of the mass-energy density of the universe can be attributed to dark energy the so called cosmological constant. It may not be less than zero or equal to zero $(\Lambda \leq 0)$, but in practice always greater than zero $(\Lambda > 0)$. This cosmological constant is understood as the fundamental force of nature in the particle physics (Felix 2012), while the modern field theory defines the cosmological constant as energy density of the vacuum. The universe contains a bizarre form of matter/energy, which is gravitationally repulsive and hence, it is an anti-gravity effect. Due to this effect, the galaxy is moving from us and the universe is expanding as shown by Hubble (Turner 2001).

There are so many experimental evidences and data available from different research papers and literatures that the gravitational constant (G) vary with time and we obtain that $\dot{G}/G = 10^{-12}$ per year is the condition that has to be satisfied in order not to cause a conflict with the observation. As per the model for variation limit of $\dot{G}/G = 10^{-12}$ per year, the radius changes by about 1% and the luminosity by 3% at the solar stage (Wang 1991). The Newtonian universal constant (G) has vital role of coupling constant between geometry of space and matter content in Einstein's field equation (Singh 2006). Dirac (1937) first proposed the idea regarding the variation of gravitational constant with time which gives a good understanding of cosmology and particle physics (Dirac 1937). Dicke (1961) gave a gravitational theory with a cosmic time increasing scalar field $\phi(t)$ which is the inverse of decreasing gravitational constant (G) i.e. $\phi(t) \propto 1/G(t)$ (Dicke 1961). Shapiro et al. (1971) discussed about the problem of gravitational constant and its variation $(\sigma)$ with cosmic time and possible experimental bound (Shapiro et al. 1971). Canuto et al. (1977) gave many suggestions based on different arguments that G is indeed time dependent (Canuto et al. 1977). Dyson (1978) proposed that G does change with a rate of variation that should be of order of the expansion rate of the universe $G/\dot{G} = \sigma H_0$, where $H_0$ is the Hubble parameter ($H_0$=2x10$^{-10}$) and $\sigma$ is a dimensionless parameter (Dyson 1978). Beesham (1986) studied the creation with variable G and pointed out that the variation of G with cosmic time as: $G \propto 1/t$ originally proposed by Dirac in 1937 (Beesham 1986). Halpern (1987) collected several works on the measurement of cosmological variations of the gravitational constant (Halpern 1987). Berman (1992) generalised the large number of hypothesis regarding the cosmological constant and concluded that the cosmological constant is the time dependent scalar field and inversely proportional to the square of cosmic time ($\Lambda = c/t^2$), where c is the proportionality constant (Berman 1992).

**The Robertson-Walker Line Element for a Spatially Homogeneous and Isotropic Medium**

The Robertson-Walker line element for a spatially homogeneous and isotropic medium is given by the following equation (Singh 2006).

$$ds^2 = dr^2 - R^2(t)\left[\frac{dr^2}{1-kr^2} + r^2\left(d\theta^2 + \sin^2\theta\right)d\phi^2\right] \quad (14)$$

where R(t) is the scale factor.

When k=-1 represents the curvature parameter for open universe and the above equation takes as

$$ds^2 = dr^2 - R^2(t)\left[\frac{dr^2}{1+r^2} + r^2\left(d\theta^2 + \sin^2\theta\right)d\phi^2\right] \quad (15)$$

When k=1 represents the curvature parameter for closed universe and the above equation takes as

$$ds^2 = dr^2 - R^2(t)\left[\frac{dr^2}{1-r^2} + r^2\left(d\theta^2 + \sin^2\theta\right)d\phi^2\right] \quad (16)$$

When k=0 represents the curvature parameter for flat universe and the above equation takes as

$$ds^2 = dr^2 - R^2(t)\left[dr^2 + r^2\left(d\theta^2 + \sin^2\theta\right)d\phi^2\right] \quad (17)$$

The Einstein field equation with variable cosmological and gravitational constants are given by the following equations

$$R_{\mu\nu} - \frac{1}{2}g_{\mu\nu}R = 8\pi G(t)T_{\mu\nu} + \Lambda(t)g_{\mu\nu} \quad (18)$$

The term $R_{\mu\nu}$ is the Ricci tensor, $g_{\mu\nu}$ be the metric tensor and R be the tensor of the scalar curvature in the left hand side of above equation. These all terms describe the properties of space time. The term $T_{\mu\nu}$ in the right hand side of the above equation represents energy momentum tensor of a perfect fluid given by the following equation

$$T_{\mu\nu} = -pg_{\mu\nu} + (p+\rho)u_\mu u_\nu \quad (19)$$

where $\rho$ is the energy density of the cosmic matter, p is the pressure and u is the four-velocity vector such that $u_\mu u_\nu = 1$

The co-variant divergence of the equation (5), taking account the Bianchi identity gives

$$8\pi G(t)T_{\mu\nu} + \Lambda(t)g_{\mu\nu} = 0 \tag{20}$$

This equation also may be considered as the fundamental equation of gravity with gravitational constant (G) and cosmological constant ($\Lambda$) in addition to the equation (5).

The Einstein field equation containing the speed of light (c) can be written as

$$R_{\mu\nu} - \frac{1}{2} g_{\mu\nu} R = \frac{8\pi G(t)}{c^4} T_{\mu\nu} + \Lambda(t) g_{\mu\nu} \tag{21}$$

The general relativity does not account G and gives no theoretical explanation like the fundamental quantity speed of light c, although G is treated as fundamental constant in nature.

According to the energy momentum conservation equation (Singh and Agrawal 1993), we have

$$T_{\mu\nu} = 0 \tag{22}$$

Putting the above value in equation (8), we have

$$R_{\mu\nu} - \frac{1}{2} g_{\mu\nu} R = \Lambda(t) g_{\mu\nu} \tag{23}$$

or

$$R_{\mu\nu} = \frac{1}{2} g_{\mu\nu} R + \Lambda(t) g_{\mu\nu} \tag{24}$$

or

$$R_{\nu\nu} = \left( \Lambda + \frac{R}{2} \right) g_{\mu\nu} \tag{25}$$

When the Hubble parameter ($H = \dot{R} / R$) is used to solve the Einstein Field equations(1) using co-moving coordinates given by the following equation

$$u_k = (1, 0, 0, 0) \tag{26}$$

Then we obtain the following results as follows:

$$H^2 + \dot{H} = -\frac{4\pi}{3} G(t)(3p + p) + \frac{1}{3}\Lambda(t) \quad (27)$$

$$H^2 = \frac{8\pi}{3} G(t)\rho + \frac{1}{3}\Lambda(t) - \frac{k}{R^2} \quad (28)$$

Let us assume that

$$G(t) = \alpha H \quad (29)$$

and

$$\Lambda(t) = \beta H^2 \quad (30)$$

where $\alpha$ and $\beta$ are dimensionless positive constants.

Then the solution of Einstein field gives the following physical parameters

$$H = \frac{3}{\left[(1-2a)\beta + 3\right]}\left(\frac{1}{t}\right) \quad (31)$$

$$G = \frac{3\alpha}{\left[(1-2a)\beta + 3\right]}\left(\frac{1}{t}\right) \quad (32)$$

$$\Lambda = \frac{9\beta}{\left[(1-2a)\beta + 3\right]^2}\left(\frac{1}{t^2}\right) \quad (33)$$

$$\rho = \frac{3(3-\beta)}{8\pi\alpha\left[(1-2a)\beta + 3\right]}\left(\frac{1}{t}\right) \quad (34)$$

and

$$R = R_*\left[(1-\beta)\left(\frac{A}{1-A}\right)^{2\beta/3} H_* t\right]^{1/(1-\beta)} \quad (35)$$

where $a$ is the free parameter related to the power of cosmic time and lies $0 \le a < 1$. $R_*$ is the reference value such that if $R \le R_*$

From the observation of above equations, we see that for the positive values of Hubble parameter, gravitational constant, cosmological constant and energy density, both the dimensionless parameters $\alpha$ and $\beta$ are should be as follows:

$$(\alpha \leq 1/2) \ \& \ \beta < 3 \tag{36}$$

When $\beta = 0$, then the equation (35) can be written as follows:

$$R = R_0 H_0 t \tag{37}$$

or

$$R \propto t \tag{38}$$

The above equation shows the radius of curvature increases linearly with the age of time at $\beta = 0$.

The variation of gravitational constant and energy density with the cosmic time using equations (32) & (34) clearly shows that the gravitational constant as well as energy density will be collapsed, when cosmic time tends to infinity.

But when each Bianchi type model (I to IX) is applied to the Einstein field equation, then we obtain the following solutions for radius of curvature, Hubble parameter, gravitational constant, cosmological constant and energy density respectively:

$$R \propto t^3 \tag{39}$$

$$H \propto \frac{1}{t} \tag{40}$$

$$\Lambda \propto \frac{1}{t^2} \tag{41}$$

$$\rho \propto \frac{1}{t} \tag{42}$$

$$G \propto \frac{1}{t} \tag{43}$$

Chen and Wu (1990) suggested that the cosmological constant $(\Lambda)$ vary as the square of the scale factor R in the Robertson-Walker model as per the following relation (Chen and Wu 1990).

$$\Lambda \propto \frac{1}{R^2} \tag{44}$$

The above relation shows that the cosmological constant decreases with increase of the radius of curvature.

The equation (39) shows that the curvature of the space increases with the cosmic time, while the equations (40), (41), (42) & (43) show that the Hubble parameter, gravitational constant and energy density decrease with the increase of cosmic time and for infinite time, the gravitational constant will be collapse and

hence no gravity will act at that time. But when we go in the reverse direction, then these models $G \propto 1/t$, $\Lambda \propto 1/t^2$ and $\Lambda \propto 1/R^2$ become singular at t=0. (Singh and Agrawal 1993, Davis and Griffen 2010, Felix 2012). This fact gives the evidence in support to the Big-Bang theory for the evolution of universe, because, the universe was a singular point at t=0.

**Hypersurface-Homogenous Dark Energy Model with Variable $E_oS$ Parameter in f(R,T) Gravity**

The line element for the hypersurface homogenous space time is given by

$$ds^2 = dt^2 - A^2(t)dx^2 - B^2(t)[dy^2 + \Sigma^2(y,K)dz^2] \quad (45)$$

where K=1, 0, -1 as discussed in equations (15), (16) and (17) in the subsection 6.1.

When the above equation is solved with proper mathematical operation for suitable choice of co-ordinates and constants, we have

$$ds^2 = dt^2 - (\alpha_1 t + \alpha_2)^{6n/m(n+2)}dx^2 - (\alpha_1 t + \alpha_2)^{6/m(n+2)}[dy^2 + \Sigma^2(y,K)dz^2] \quad (46)$$

This model has no initial singularity and represents hypersurface-homogenous Dark energy model in f(R,T) gravity.

This model gives the parameters like the spatial volume (v), the generalised Hubble parameter (*H*), scalar expansion (θ), mean isotropic parameter (Λ), shear scalar (σ), energy density (ρ) and equation of state & Skewness parameter (ω) respectively as follows:

$$V = (\alpha_1 t + \alpha_2)^{3/n} \quad (47)$$

$$H = \alpha_1 / m(\alpha_1 t + \alpha_2) \quad (48)$$

$$\theta = 3\alpha_1 / m(\alpha_1 t + \alpha_2) \quad (49)$$

$$\Lambda = 3(n^2+2)/(n+2)^2 \quad (50)$$

$$\rho = \frac{1}{(8\pi + 2\mu)}\left[\frac{3\alpha_1^2(n+1)(3-mn-2m) + 9\alpha_1^2(n^2-2n-1)}{m^2(n+2)^2(\alpha_1 t+\alpha_2)^2} - \frac{K}{\{(\alpha_1 t+\alpha_2)\}^{6/m(n+2)}}\right] = -p \quad (51)$$

$$w = \frac{1}{\rho(8\pi + 2\mu)}\left[\frac{3\alpha_1^2(3-mn-2m) - 3n\alpha_1^2(3n-mn-2m) + 9\alpha_1^2}{m^2(n+2)^2(\alpha_1 t+\alpha_2)^2} - \frac{K}{\{(\alpha_1 t+\alpha_2)\}^{6/m(n+2)}}\right] = -\delta \quad (52)$$

The equation (47) shows that the spatial volume of the universe increases with increasing cosmic time and gives the accelerated expansion of the universe. The equation (48) shows that the Hubble parameter decreases with increasing cosmic

time and gives the null value of H for infinite cosmic time. The equation (49) shows that the expansion scalar decreases with increase of the cosmic time. The equation (50) shows that the mean anisotropic parameter is uniform throughout the evolution of the universe, because it is independent of cosmic time. The equation (51) shows that in the beginning of the universe the shear scalar was infinitely large and with increasing the cosmic time, it initially decreases rapidly to reach null value as the cosmic time tends to infinity. The equation (52) represents the equation of state and Skewness parameter depends on the cosmic time. The parameter $E_OS$ remains the same from beginning to till time, but it acquires different positions for K= -1,0 , 1. These all variations of the parameters like *V*, *H*, $\theta$, $\rho$ and $\omega$ with cosmic time are shown graphically in the reference (Shaikh and Wankhade 2015).

## Line Element from a GW from Standard General Relativity

The line element for a gravitational arising from standard general relativity and propagating in the z direction using natural units equal to unity is given by following equation

$$ds^2 = dt^2 - dz^2 - (1+h_+)dx^2 - (1-h_+)dy^2 - 2h_\times dxdy \qquad (53)$$

where $h_+$ and $h_x$ are the weak perturbations due to the (+) and (x) polarisation.

The total frequency and angle dependent response function to the (+) and (x) polarisation of an interferometer with arms in the u and v directions w.r.t. the propagating gravitational waves are given as follows:

$$H_+(w) = \frac{\cos^2\theta\cos^2\phi - \sin^2\phi}{2L} H_u(w,\theta,\phi) - \frac{\cos^2\theta\sin^2\phi - \cos^2\phi}{2L} H_v(w,\theta,\phi) \qquad (54)$$

and

$$H^\times(w) = \frac{-\cos\theta\cos\phi\sin\phi - \sin^2\phi}{L}[H_u(w,\theta,\phi) - H_v(w,\theta,\phi)] \qquad (55)$$

In the case of low frequency limit ($w \to o$), the low frequency response functions tend to the low values for both the equations (54) & (55).

The total frequency and angle dependent response function of an interferometer to this scalar polarisation is given by the following equation.

$$H^\phi(w) = \frac{\sin\theta}{2i\omega L}\{\cos\phi[1+\exp(2i\omega L) - 2\exp i\omega L(1+\sin\theta\cos\phi)] - \sin\phi[1+\exp(2i\omega L) - 2\exp i\omega L(1+\sin\theta\sin\phi)]\} \qquad (56)$$

If the interferometer arm is parallel to the propagating gravitational wave, the longitudinal response function with the bouncing photon analysis associated with such a massive mode is given by the following equation.

$$T_l(\omega)=\frac{1}{m^4\omega^2 L}[1/2\{1+\exp(2i\omega L)m^2\omega^2 L(m^2-2\omega^2)-i\exp(2i\omega L)\omega^2\sqrt{-m^2+\omega^2}(4\omega^2+m^2(-1-i\omega L)\}$$
$$+\omega^2\sqrt{-m^2+\omega^2}(-4i\omega^2+m^2(i+\omega L)+\exp iL(\omega+\sqrt{-m^2+\omega^2})(m^6L+m^4\omega^3 L$$
$$+8i\omega^4\sqrt{-m^2+\omega^2}+m^2(-2\omega^4 L)-2i\omega^2\sqrt{-m^2+\omega^2})\}$$
$$+2\exp(i\omega L)\omega^3(-3m^2+4\omega^2)\sin(\omega L)] \quad (57)$$

The theory of gravitation as per general relativity admits only two response functions (54) and (55) corresponding to the two canonical polarisations $h_+$ and $h_x$ respectively and concludes that the general relativity is definitive. If the third polarisation is present, the third response function (57) will be detected by the gravitational wave interferometers.

Astronomers have made a new detection of gravitational waves and for the first time have been able to trace the shape of ripples sent through spacetime when black holes collide. Three scientists named: Rainer Weiss, Kip Thorne and Barry Barish jointly awarded by Nobel prize (2017) for the detection of gravitational waves coming from the collision of two massive black holes situated a billion light years away from us as predicted by Albert Einstein 100 years ago (Delvin 2017). The detection of the gravitational wave rules out the general relativity as definitive theory of gravity. Hence the presence of a longitudinal response function (equation 57) for a wave propagating parallel to one interferometer arm gives that the correct theory of gravity is massive scalar-tensor gravity (Corda 2009).

## Dark Matter and Dark Energy

In physical cosmology, dark energy is a hypothetical form of energy that permeates all of space and tends to increase the rate of expansion of the universe. The modern concept regarding the history of observable universe is broadly divided into three stages (David 1993). Inflationary era, Radiation dominated era and Matter dominated era.

Naturally, the dark energy is diffuse and a low-energy phenomenon. It is probably, neither found in galaxies nor in the clusters of galaxies and can't be produced at accelerators. The Universe itself is perhaps only the natural laboratory in which we can study it (Turner 2001). The observation shows that the universe is expanding and contains about 75% dark energy, 20% dark matter and 5% normal (atomic) matter, with smaller contributions from photons and neutrinos (Caldwell and Kamionkowski 2009). There is some compelling evidence that about 90% of the mass of the Universe is invisible. This fact was explained by Oort during the analysis of Doppler shift in the spectra of stars in the galactic disk. He also concluded that the amount of gravitating matter implied by the measured velocities could not be explained by the mass of visible stars. This gives the evidence the presence of invisible matter. He also studied that a large spherical collection of

stars called globular clusters move within the galaxy too fast to be bound to the galaxy by the gravitational influence of the luminous matter alone and half of the Galaxy disk was made of dark matter before astronomers decided to investigate the problem further (Freeman and McNamara 2006). Zwicky (1933) concluded that the velocity dispersion in rich clusters of galaxies require a huge amount of mass to keep them bound could be accounted by the luminous galaxies themselves, when he was observing the Coma Cluster of galaxies (Zwicky 1933). The matter and energy used to keep bound the luminous galaxies are known as dark matter and energy. The most new burning and revolutionary topics for research in the cosmology and astronomy is dark matter and dark energy. Ram and Chandel (2014) have shown that the universe exhibits transition from deceleration to acceleration (Ram and Chandel 2014). Reddy and Kumar obtained Bianchi type II cosmological model and an exact cosmological model with an appropriate choice of the function f(RT) (Reddy and Shanthi 2013). Rao and Davuluri (2014) gave the solution of the field equations to use the anisotropy feature of the universe in the Bianchi type-VI 0 space time (Rao and Davuluri 2014). Singh & Singh obtained a model of the universe containing some part of quintessence form of dark energy and some part of cosmological constant form of dark energy and found that this new model is viable form of model of the universe consisting of dark energy (Singh and Singh 2014).

**New Cosmology and Dark Energy**

The New Standard Cosmology is characterised by the following features (Mathews et al. 2017). It is flat and accelerating Universe with early period of expansion (inflation).

1. It has inhomogeneous density produced from quantum fluctuations during inflation.
2. It consists of 2/3rds dark energy; 1/3$^{rd}$ dark matter; 1/120$^{th}$ bright stars.
3. Matter content: $(29 \pm 4)\%$ cold dark matter; $(4 \pm 1)\%$ baryons and 0.3% neutrinos.

The above model for New Cosmology is certainly not as well established as the standard hot big bang. However, the evidence is mounting.

Dark energy is a cosmological term for the causative agents of the current epoch of accelerated expansion. The dark energy has following defining properties:

i. It emits no light.
ii. It has large negative pressure.
iii. It is approximately homogeneous
iv. It is more “energy-like” than “matter-like”. Dark energy is qualitatively very different from dark matter.

v. Dark energy by its nature is diffuse and a low-energy phenomenon.

vi. It probably cannot be produced at accelerators.

vii. It is a mysterious substance with negative pressure and accounts for nearly 70% of the total matter-energy of the universe, but has no clear explanations.

viii. It is not very dense.

ix. There is a possibility that dark energy may become dark matter when buffeted by baryonic particles.

## Some Challenges to the Dark Energy

The New Standard Cosmology leaves some burning questions as follows:

1. What is physics underlying inflation?
2. What is the dark-matter particle?
3. How was the baryon asymmetry produced?
4. What is the nature of dark energy?

Regarding this context, the physicists and researchers associated with astrophysics and astronomy should take it as a challenge to solve all these questions so that an exact solution about the dark energy problems is solved.

## Results and Discussion

In the present work, we have studied different existing models of dark matter and energy for the universe evolution as proposed by many cosmology and astronomy researchers. Out of these different models, each Bianchi type models (I to IX) is applied to the Einstein field equation with the principle of conservation of energy, gives that the universal constant or gravitational constant is inversely proportional to the cosmic time for which the model finally becomes singular at t=0.

We know that at the time of Big Bang, the universe was also singular at zero time. From that time, the universe is expanding like balloon in all possible outward directions from the beginning point of the Big Bang/explosion of the primordial black hole. The universe contains $10^{11}$ galaxies and each galaxy has $10^{11}$ stars. Due to the expansion of universe, all the galaxies together with their stars are moving or receding from us. This will give rise the Doppler shift/red shift due to the spectra of stars in the galactic disk which can determine the distance of the galaxy/star from us. As per the relation $\Lambda \propto t^{-2}$ and $G \propto t^{-1}$, on increasing the value of the cosmic time(t), the cosmological constant as well as gravitational

constant will decrease and finally, when this cosmic time will approach to the infinity, both the constants will vanish.

At this stage, the spatial volume of the universe becomes enough large acquiring its extreme values as is clear from equation (47). The expansion scalar function, shear scalar function and energy density all tend to zero and no change takes place in the mean isotropic parameter. The energy density gives the negative pressure as predicted by equation (52) justifying the property of dark energy.

This will lead the stoppage of the expansion of the universe and shear will die out. Hence, an unbalanced position will be reached and anti-gravity will fail to act and hence the contraction of the universe may start and after billions and billions years, the shape of the universe will become an egg like. After acquiring the certain limit of the shape of the universe like an egg, another Big Bang will happen and hence in his way, the new universe will form.

The theory of gravitation as per general relativity indicated by equations (54) and (55) for two canonical polarisations $h_+$ and $h_x$ respectively concludes that the general relativity is definitive. But when the third polarisation is present indicating the third response function (57) will rule out the general relativity as definitive theory of gravity and gives that the correct theory of gravity is massive scalar-tensor gravity.

From whole study of this work, we conclude that the variation of Gravitational constant, cosmological constant, spatial volume, expansion shear, expansion scalar, energy density with the cosmic time have vital responsibility to hold in balancing the position of the universe together with their galaxies and stars by invisible matter and energy so called dark matter and dark energy.

## Conclusions

The fact of dark matter and dark energy explains the evolution of the universe and gives some evidences in the support of expanding universe and is also concluded that the variation of the both gravitational and cosmological constants with the cosmic time have vital responsibility to hold in balancing position of the universe together with their galaxies and stars. The detection of the gravitational waves from collision of binary black holes shows that the massive scalar-tensor gravity is definitive theory of gravity drawn from the detection of gravitational wave coming from the collision of binary black holes.

## Acknowledgements

We are obliged and thankful to reviewers who found out the shortcomings in the original manuscript and gave some important suggestions to make it better.

## References

A142 (2012) *Black holes*. Winter.
Aguirre A (2008) *Dark matter in cosmology*. WSPC Proceedings.
Beesham A (1986) Variable-*G* cosmology and creation. *International Journal of Theoretical Physics* 25(12): 1295–1298.
Berman MS (1992) Generalized large number hypothesis and cosmological constant. *International Journal of Theoretical Physics* 31(7): 1217–1219.
Bilic N (2010) Thermodynamic properties of dark energy. *Progress of Physics* 56(4-5): 363–372.
Bilic N (2011) Supersymmetric dark matter. Retrieved from: https://www.slideshare.net/seenet/n-bilic-supersymmetric-dark-energy.
Boyle LA, Caldwell RR, Kamionkowski M (2002) "Spintessence! New Models for Dark Matter and Dark Energy. *Physics Letters B* 545(1-2): 17–22.
Buchert T (2008) Dark Energy from structure: a status report. *General Relativity and Gravitation* 40(2-3): 467–527.
Caldwell R, Kamionkowski M (2009) Cosmology: dark matter and dark energy. *Nature* 458(7238): 587–589.
Canuto VM, Adams PJ, Hsieh SH, Tsiang E (1977): Scale-covariant theory of gravitation and astrophysical applications. *Physical Review D: Particles and Fields* 16(6): 429–432.
Chen W, Wu YS (1990) Implication of a cosmological constant varying as $R^{-2}$. *Physical Review D* 41(2): 695–698.
Chiba T (2011) The constancy of the constants of nature: updates. *Progress of Theoretical Physics* 126(6): 993–1019.
Coc A, Vangioni E (2017): Primordial nucleosynthesis. *International Journal of Modern Physics E* 26(8): 1–35.
Corda C (2009) Interferometric detection of gravitational waves: the definitive test for general relativity. *International Journal of Modern Physics D* 18(14): 2275–2282.
Dallal SA, Azzam WJ (2012) On supersymmetry and the origin of dark matter. *Journal of Modern Physics* 3(9): 1131–1141.
Davis T, Griffen B (2010) Cosmological constant. *Scholarpedia* 5(9): 4473.
Delvin H (2017) *New gravitational wave detection shows shape of ripples from black hole collision, science correspondent*. The Guardian. Retrieved from: https://www.theguardian.com/science/2017/sep/27/new-gravitational-wave-detection-shows-shape-of-ripples-from-black-hole-collision-ligo-virgo.
Dicke RH (1961) Dirac's cosmology and Mach's principle. *Nature* 192 (4801): 440–441.
Dirac PAM (1937) The cosmological constants. *Nature* 139(3512): 323.
Dyson FJ (1978) Variations of constants. In JE Lannutti, PK Williams (Eds), 163–167. *Current Trends in the Theory of Fields*. New York: American Institute of Physics.
Freeman K, McNamara G (2006) *In search of dark matter*. UK: Springer.
Halpern L (1987) *On the measurement of cosmological variations of the gravitational constant*. Gainesville: University Presses of Florida.
Hubble EP (1926) A spiral nebula as a stellar system: Meissner 33. *Astrophysical Journal* 63(May): 236–274.
Hubble EP (1929) A relation between distance and radial velocity among extra-galactic nebulae. *Proceeding of the National Academy of Science* 15(3): 168–173.
Hubble EP (1982) *The realm of the nebulae*. Yale University Press.
Kahn FD, Woltjer L (1959) *Intergalactic matter and the galaxy*. *Astrophysical Journal* 130(Nov): 705.

Kirshner RP (2004) Hubble's diagram and cosmic expansion. *Proceedings of the National Academy of Sciences* 101(1): 8–13.

Lev FM (2012) Do we need dark energy to explain the cosmological acceleration? *Journal of Modern Physics* 3(9A): 1185–1189.

Lyth DH (1993) *Introduction to cosmology*. Lectures Given at the Summer School in High Energy Physics and Cosmology, ICTP (Trieste). arXiv:astro-ph/9312022v1.

Mahto D, Nadeem MS, Prasad U, Vineeta K (2013): Study of variation of gravitational constant (G) in very strong gravitational field. *International Journal of Astrophysics and Space Science* 1(4): 56–60.

Mathews GJ, KusakabeM, Kajino T (2017) Introduction to Big Bang nucleosynthesis & modern cosmology. *International Journal of Modern Physics* 26(8): 1–21.

Melek M (2000): Universe's expansion puts limits on the cosmic time scale variations of gravitational and cosmological constants. *Astrophysics and Space Science* 272(Sep): 417–421.

Patrignani C et al. (2016) Big Bang nucleo-synthesis. *Chinese Physics C* 40(Oct): 1–15.

Planck Collaboration (2016) *Astronomy & astrophysics* 594(A13).

Ram S, Chandel S (2014) Dynamics of magnetised string cosmological model in f(R,T) gravity theory. *Astrophysics and Space Science* 355(1): 195–202.

Rao M, Davuluri N (2014) Strange quark matter attached to string cloud in general scalar tensor theory of gravitation. *Iranian Journal of Physics Research* 14(13): 35–39.

Reddy DRK, Shanthi K (2013) LRS Bianchi Type – II Universe in F(R,T) Theory of Gravity. *Global Journal of Science Frontier Research* 13(2): 23–27.

Shaikh AY, Wankhade KS (2015) Dark energy cosmological model in f(R, T) gravity. *Prespacetime Journal* 6(11): 1213–1229.

Shapiro II, Smith WB, Ash MB, Ingalls RP, Pettengill GH (1971): Gravitational constant: experimental bound on its time variation. *Physical Review Letters* 26(1): 27–30.

Silva R, Goncalves RS, Alcaniz JS, Silva HHB (2011) *Thermodynamics and dark energy*. arXiv:1104.1628v1[astro-ph.CO].

Singh CP (2006) Early Universe with variable gravitational and cosmological constants. *International Journal of Theoretical Physics* 45(3): 531–540.

Singh KM, Singh KP (2014) Cosmological model universe consisting two forms of dark energy. *International Journal of Theoretical Physics* 53(12): 4360–4365.

Singh T, Agrawal AK (1993) Homogenous anisotropic cosmological models with variable gravitational and cosmological constants. *International Journal of Theoretical Physics* 32(6): 1041–1059.

Staff (2019) *How many stars are there in the universe?* European Space Agency.

Turner MS (2001) *Dark energy and the new cosmology*. arXiv:astro-ph 0108103v1.

Wang J (1991) Astrophysical constants on the gravitational constant. *Astrophysics and Space Science* 184: 31–36.

Zwicky F (1993) On the metric of space time. *Helvetca Physica Acta* 6: 110–125.